Batteries & Supercaps

Review
doi.org/10.1002/batt.202400302

Chemistry Europe
European Chemical Societies Publishing

www.batteries-supercaps.org

Eco-friendly Anode Materials for Lithium and Sodium-ion Batteries from Wood Sources

Junaid Aslam,[a] Muhammad Ahsan Waseem,[a] Yifan Zhang,[a] and Yong Wang*[a]

The intricate materials found in nature boast remarkable multifunctional properties honed through millions of years of evolution, resulting in the highest optimal organization in terms of function, structure, and chemistry. Leveraging the distinctive attributes of natural materials through biomimicry present a captivating avenue for research, brimming with vast potential for groundbreaking discoveries. Among the array of precursors available, wood stands out as a prominent candidate that covered over 30% of the global land surface. Renowned for its captivating mechanical properties and anisotropic hierarchical porosity finely tuned to facilitate swift pathways, wood embodies attributes of abundance and biodegradability. Consequently, scientists have drawn inspiration from wood's exceptional characteristics to engineer batteries exhibiting remarkable electrochemical performance. For instance, the characteristic hierarchical multi-channeled construction of wood serves as a blueprint for synthesizing energy storage materials endowed with heightened ion and electron diffusivity. Serving as an integrated carbonaceous scaffold featuring a hierarchical architecture and aligned channels, wood-based anodes enhance ion and electron conductivities, while bolstering the kinetics of charge transfer in lithium-ion batteries (LIBs) and sodium-ion batteries (SIBs). This review underscores the recent strides made in utilizing wood as a hierarchically porous and renewable material for developing anode materials tailored for LIBs and SIBs. Additionally, it sheds light on the potential of wood-derived anode materials for LIBs and SIBs to alleviate the strain on critical raw materials, while accentuating the additional environmental sustainability benefits derived from such innovations.

1. Introduction

With over 8 billion in population, the demand for energy escalates at a disquieting pace. Given the escalating reliance on the over-exploitation of fossil fuels within an expanding world populace, there emerges a pressing imperative to embrace sustainable energy sources in order to meet the burgeoning expectations for power in our contemporary way of life.[1,2] The imperative to develop cost-effective, renewable, and sustainable energy storage systems with elevated energy and power density has become increasingly pressing due to the reduction of global natural resources and the escalating environmental catastrophe. In response, cutting-edge batteries have emerged as a crucial solution, offering exceptional safety, prolonged cycle life and power output. Among these innovative energy storage solutions, lithium-ion batteries (LIBs) have established themselves as the pioneering technology while spearheading a paradigm shift in the energy sector.[1,3,4] As an illustration, the global grid-battery energy storage market is projected to witness a growth rate of 23% per annum or potentially higher by the year 2030. Lithium (Li) remains a highly scarce resource within the Earth's crust, constituting merely 0.0017 wt.%, and its mining deposits are predominantly located in politically volatile regions.[5] Hence, attention has shifted towards the advancement of energy storage systems utilizing abundant and viable elements, notably sodium-ion batteries (SIBs), which are deemed as the prime candidate to supplant LIBs. For stationary applications such as wind energy storage systems, the transition from LIBs to SIBs is of utmost importance. Sodium (Na) presents itself as a more economical and plentiful alternative to lithium (Li), boasting an estimated 2.8 wt.% of total Na concentration globally.[6,7]

In addition, carbon nanotubes and graphene emerge as promising alternatives.[8,9] Nevertheless, these carbon-based materials confront formidable challenges, including high cost production, intricately complex fabrication processes at large scale as well as unsustainable methodologies. Innovative solutions are required to overcome these hurdles and unlock the full potential of advanced battery technologies.[10] Consequently, there exists a pressing imperative to pioneer novel carbon-based functional materials that are cost-effective and amenable to scalable synthesis methodologies.[11,12] Given the assertion, carbonaceous anode materials sourced from wood reservoirs have sparked substantial intrigue which is attributed to their facile manipulation, inherent non-toxicity, global availability and the copiousness of wood reservoir.[13–17] As a result of exceptional cycling stability along with rate performance carbon materials derived from wood can be effectively transformed into porous configuration for their use in battery. With considerable number of scientific publications over the last ten years in order to develop bio-based electricity storage devices scientists and engineers from all over the world are contributing to this cause.[14,16,18] For batteries applications plenty of research has been dedicated to wood derived materials as anodes.[13,14] The primary benefits of employing

[a] J. Aslam, M. Ahsan Waseem, Y. Zhang, Y. Wang
Department of Chemical Engineering, School of Environmental and Chemical Engineering, Shanghai University, 99 Shangda Road, Shanghai 200444, People's Republic of China
Tel: +86-21-66137723
Fax: +86-21-66137725
E-mail: yongwang@shu.edu.cn

wood-derived carbon anodes in batteries can be distilled into several key attributes, including (i) expansive interlayer spacings that afford exceptional mechanical and physical stability during the process of intercalation/de-intercalation of ions, and (ii) enhanced charge transfer efficiency as a result of abundant and diverse surface functionalities;[19] (iii) Notable features encompass a high specific surface area (SSA), finely honed pore structures exhibiting varied nano-scales, and commendable thermal stability, facilitating swift mass transport; (iv) the configuration and surface of wood-derived carbons lend themselves readily to modification or tailoring, including alterations to their chemical composition and surface functionalities, such as heteroatom doping (e.g., Nitrogen, Oxygen, Sulphur). Hence electrochemical performance metrics such as longevity, safety as well as capacity are increased;[20] and (v) the better accessibility of wood is another key attribute that refers to the ease of obtaining carbon materials from wood. It suggests that there are various types of wood-derived carbon materials that are readily accessible.[15–17] Materials derived from wood emerge as paramount contenders for the forthcoming generation of anodes in LIBs and SIBs. Wood-derived materials have garnered substantial scrutiny as potential anode candidates for both LIBs and SIBs.[21] Anode materials derived from wood undoubtedly stand as a naturally abundant, inexhaustible, and environmentally friendly energy reservoir on the planet, ripe for exploitation across both fundamental research and applied domains within the realms of LIBs and SIBs.[22] The inherent attributes of wood, such as its renewability, mechanical integrity, and flexibility, are underscored as key factors rendering it ideally suited for diverse applications within LIBs and SIBs.[23,24] Both offer potential advantages and continue to evolve, with ongoing research focused on enhancing their performance for various applications.[25] Hence, there exists a compelling allure in exploring energy storage materials directly sourced from trees, which hold promise for a wide array of battery applications, as illustrated in Figure 1(a). Fortuitously,

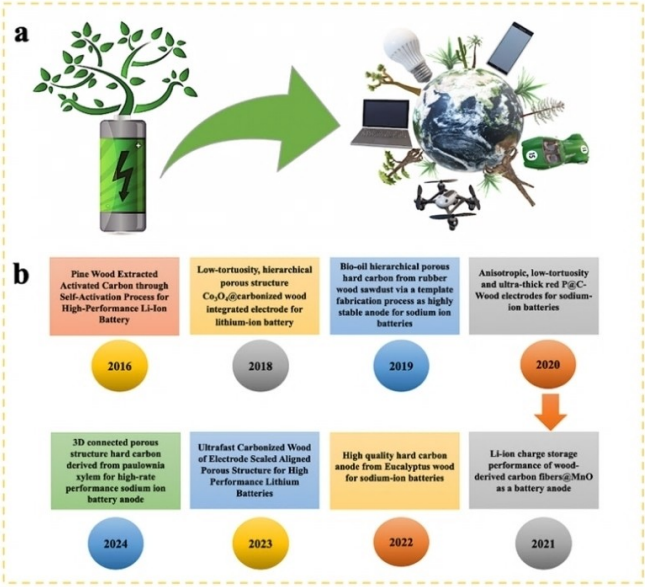

Figure 1. a) The schematic representation of wood-based battery applications. b) developments in wood-based anode materials in energy storage systems, illustrated via case studies.

the inherent layers of wood anodes, boasting natural mechanical strength and flexibility, serve to mitigate issues such as cracking or delamination from the current collector. Wood-based anode materials possess a hierarchical porous structure, which offers numerous active sites for ion and electron storage and transfer. This structure provides a favorable environment for efficient ion and electron transport, minimizing the time these charge carriers spend shuttling between active sites.[26] As a result, the internal resistance of the battery is reduced. The reduced shuttle time of ions and electrons within the wood anode material translates into improved rate performance of the battery.[27] Rapid ion and electron transport enables the

Junaid Aslam is currently pursuing his doctoral studies at Shanghai University under the guidance of Professor Yong Wang. He completed his master's degree from Shanghai University in 2023. His research interests focus on the energy storage materials for alkali metal-ion batteries.

Muhammad Ahsan Waseem is currently pursuing a doctoral degree at Shanghai University, where he is working as a researcher under the guidance of Professor Yong Wang. In 2013, he completed his master's degree from Karlstad University, Sweden. His current academic research centres around the development and fabrication of energy storage materials for various applications such as (LIBs), (KIBs), and supercapacitors (SCs).

Yifan Zhang received his Ph.D. in catalytic engineering at the Inha University, South Korea in 2020 and subsequently joined the School of Environmental and Chemical Engineering at Shanghai University and was appointed as an associate professor in 2020. Currently, Dr. Zhang's research direction mainly focuses on nanomaterials and their applications in the field of photo electrocatalysis.

Yong Wang completed his Ph.D. in Chemical Engineering at the National University of Singapore in 2004. Following this, he served as a research fellow at the Singapore-MIT Alliance from 2004 to 2006. In 2007, he joined Shanghai University as a professor. His research primarily centres on materials for energy storage and environmental applications.

battery to charge and discharge more effectively, even under high current densities. The efficient ion and electron transport in wood-based anode materials contributes to higher energy density in the battery. By minimizing energy losses associated with internal resistance, more of the stored energy can be effectively utilized during charging and discharging cycles. This allows for greater energy storage capacity within the same volume or mass of the battery, leading to increased energy density.[28] Hence, ions and electrons require less time to traverse to active sites across the comprehensive wood anodes, resulting in reduced cell resistance, heightened rate capability, and energy density.[29] Remarkable strides have been made in the realm of wood-derived energy storage devices over the past decades, portending a promising future for wood anodes in both LIBs and SIBs. Additionally, Figure 1(b) delineates the significant evolution, development, and milestones of wood-derived materials as anode for LIBs and SIBs.[30] In the pursuit of high-performance and optimal anode materials for lithium-ion and sodium-ion batteries (SIBs), it becomes imperative to fine-tune the essential and significant properties of wood carbon anode materials, including structural defects, porosity, interlayer spacing and pore structure, as well as the number and type of functionalities. Utilizing carbon anode materials derived from wood offers a pathway to streamline the process substantially while transitioning towards renewable and environmentally sustainable feedstock.[31]

Wood and its derivatives offer sustainable, renewable, and biodegradable materials with unique properties, making them ideal for advanced nano-technologies and a wide range of applications.[32] The future of engineering wood-based materials lies in promoting continuous progress towards true sustainability, spanning from material design to diverse applications in energy storage, wastewater treatment, and solar-steam-assisted desalination.[33] This review highlights the potential of wood-based materials for energy engineering, emphasizing their abundant, renewable, and biodegradable nature, as well as their hierarchically porous structures and tunable functionalities. Additionally, it discusses the development and progress of wood-based anodes with hierarchical architecture and aligned channels to enhance energy storage and conversion capabilities, particularly in emerging energy chemistries such as lithium-ion and sodium-ion batteries (SIBs) especially in the last four years.[34] By thoroughly examining the conversion mechanisms and structural attributes of carbon materials derived from wood, this review provides profound insights into the potential of wood-based anodes for advanced energy storage systems.

2. Contrasting Lithium-Ion Batteries with Sodium-Ion Batteries

Li and Na, the subsequent elements within Group IA, exhibit analogous physicochemical attributes. Sodium is the second lightest as well as smallest alkali metal after lithium. Hence it has emerged as an optimal alternative for LIBs owing to its comparable availability of material and standard electrode potential as shown in Table 1. Although the apparent simplicity in transitioning electrode materials from LIBs to SIBs, substantial disparities exist in chemical characteristics and performance, rendering the process far from straightforward.[35,36] Being an important anode material for LIBs, conversely in case of SIBs it has been observed that sodium intercalation is not efficient in graphite.[37] Nonetheless, upon comparison of layered oxides such as Sodium cobalt oxide ($NaCoO_2$) with the same crystal structure of Lithium Coalt Oxide ($LiCoO_2$), the discrepancy in potential reversible capacity is considerably diminished. The theoretical capacities for $LiCoO_2$ and $NaCoO_2$ are respectively calculated to be 274 and 235 mAh/g, anticipated to undergo one-electron cobalt ion redox (Co_3^+ redox).[38] With numerous distinctions, both lithium and sodium-ion batteries (SIBs) exhibit analogous electrochemical properties. Various substances, including anodes which are based on carbon, can function as a shared anode for these two battery systems.[39] Lithium-ion batteries (LIBs) stand as the firmly entrenched and predominant battery technology. It holds the mantle as the most extensively utilized energy storage system in contemporary society. In the pursuit of a more efficacious energy transition, global research endeavors are directed towards high-energy-density batteries, among which LIBs have emerged as a preeminent contender for efficient energy storage solutions.[40,41] Even with escalating costs and uncertainties regarding the sourcing of constituent materials, the popularity of LIBs continues to soar. Driven by mounting demand and an imbalanced geographical distribution, lithium (Li) and graphite (Gr) are evolving into increasingly vital strategic resources. In LIB construction, the anode comprises either $Li_4Ti_5O_{12}$ (LTO) or Gr, while cathode materials include lithium cobalt oxide (LCO), lithium iron phosphate (LFP), lithium manganese oxide (LMO), lithium nickel-manganese-cobalt (NMC), and lithium nickel-cobalt-aluminum oxide (NCA).[42]

Approximately 95% of the global production of lithium-ion batteries (LIBs) comes from Asian nations such as China, Taiwan, Japan, and South Korea. Nevertheless, widespread utilization of graphite (Gr) as anode material in LIBs, has encountered limitations in meeting requisites pertaining to energy capacity and operational reliability. Consequently, a plethora of alternative anode materials have been extensively explored and trialed to supplant Gr. These include binary transition metal oxides, tin, and silicon, as well as lithium metal for solid-state batteries. Particularly noteworthy are carbon materials that are obtained from bio-mass which boasts distinctive structure and morphologies, renowned for their propensity to exhibit height-

Table 1. Comparison of LIBs and SIBs.[52]

Metal	Na	Li
Atoms radius/Å	1.86	1.52
Ionic radius/Å	1.02	0.76
Standard electrode potential/V	−2.71	−3.04
Earth crust abundance	2.8%	0.0065%
Theoretical specific capacity/(mAh/g)	1166	3862

ened specific capacity.[43] SIBs represents a variant of rechargeable battery similar to the LIB, albeit employing sodium ions (Na^+) as the primary charge carrier. SIBs boast numerous advantages over rival battery technologies; still, comprehensive research and development endeavors remain imperative to explore their full potential.[44] Numerous enterprises are currently engaged in the development of commercially viable sodium-ion batteries (SIBs) tailored for diverse applications. SIB variants are characterized by elevated energy densities, exemplary electrochemical performance, and heightened stability. However, SIBs are yet to achieve commercial fruition, notwithstanding announcements from select companies such as CATL and BYD regarding impending production. Should the cost of SIBs undergo further reduction, they stand poised to garner preference for energy storage in grid systems, particularly in scenarios where battery mass is of negligible significance.[45] The SIBs are electrochemical energy storage devices like LIBs because both are working on the same principle (intercalation and deintercalation). Then the question is why we should concentrate on SIBs rather than LIBs, even though they have lower energy density.[46–48] The materials essential for lithium-ion batteries (LIBs), notably lithium, are inherently scarce in Earth's crust. Nonetheless, researchers are actively exploring substitute battery technologies for electric vehicles to mitigate the risk of energy catastrophes. With the anticipated surge in electric vehicle demand, there arises a corresponding increase in battery demand, potentially exacerbating supply chain challenges due to limited lithium sources. Notably, sodium-ion batteries (SIBs) have aroused as a viable solution to the scarcity of lithium, given their abundant availability and cost-effectiveness.

Consequently, there is a growing inclination towards intensifying research efforts in the realm of SIBs, as they offer promising prospects for addressing this pressing issue.[49] Sodium-ion batteries (SIBs) came into being in the early 1980s, emerging alongside lithium-ion batteries (LIBs). During this era, experimentation with the intercalation process of TiS_2 was conducted for both LIBs and SIBs. By 1990, a cost-effective graphite anode with moderate capacity was trialed for both battery chemistries. LIBs exhibited superior performance compared to SIBs, leading to the latter being overlooked. Subsequently, endeavors centered around sodium-ion batteries (SIBs) gained prominence due to their heightened energy density. Nevertheless, these devices necessitated operation at elevated temperatures (300 to 350 °C) to retain sodium in its liquid state (with a melting point of 98 °C), employing sodium β alumina solid state electrolytes as the medium for ion transport. Challenges such as poor power density, safety concerns, and logistical complexities impeded further advancement. Accordingly, the pursuit of room temperature SIBs has garnered widespread acknowledgment as a viable alternative to LIBs.[50,51] The composition of a sodium-ion battery (SIB) is comprised of an anode along with cathode, electrolyte, and a separator. The cathode plays a pivotal role in accommodating Na^+ ions reversibly at a voltage greater than 2 V vs. Na^+/Na. Within compounds that are based on oxides, Na^+ ions primarily occupy prismatic and octahedral sites. These sites have larger size, which renders them less stable in tetrahedral coordination compared to Li-ions. Conversely, polyanionic materials feature octahedral interstitials within their structures, rendering them promising candidates for cathodes in SIBs. At ambient temperatures, organic electrolytes exhibit heightened electrochemical characteristics conducive to sodium-ion batteries (SIBs). This organic solvent amalgamates ethylene carbonate (EC), Propylene carbonate (PC), Ethyl methyl carbonate (DMC), and Diethyl carbonate (DEC), combined with sodium salt $NaPF_6$. Such a composition demonstrates commendable chemical resilience, ionic conductivity, and a considerable potential window. An effective anode must operate at a lower voltage threshold (below 2 V) while effectively serving as a host for Na^+ ions.[49] The operational principles of both lithium-ion batteries (LIBs) and sodium-ion batteries (SIBs) exhibit striking similarities. In these systems, the migration of Li^+/Na^+ ions from the cathode to the anode facilitates the formation of chemical bonds, thereby storing energy during the charging phase. Redox reactions unfold at the anode and cathode throughout the charging and discharging cycles, facilitates the seamless conversion of chemical energy into electrical energy. Illustrated in Figure 2, the transportation mechanism delineates the transit of Li^+/Na^+ ions via the electrolyte and the flow of electrons through the external circuitry. The current flows from anode to the cathode during discharge, with a reversal during the charging process. The mechanisms governing lithium storage in LIBs bear remarkable resemblance to those involved in sodium storage within SIBs.[39]

3. Structural Characteristics of Wood

The structural composition of timber derived from natural forests exhibits anisotropic properties owing to the inherent

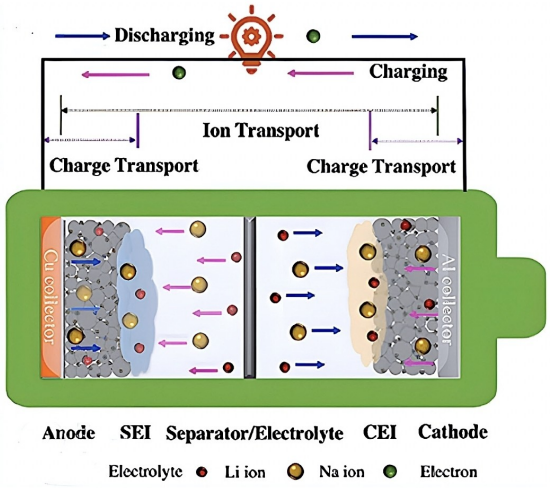

Figure 2. The schematic representation of kinetics of ions/electron in LIB/SIB. Adapted from Ref.[39] Copyright (2023) with permission from Wiley online library.

biological diversity, particularly attributable to the myriad species present, rendering it notably more intricate compared to homogeneous bulk materials. Wood cells typically organize themselves in two distinct configurations: one aligning parallel to the trunk, exemplified by the elongated axial cells, and the other dispersed radially from the heartwood to the bark, typified by the ray cells.[53,54] The hierarchical channel is renowned for its capacity to provide conduits for the movement of water, nutrients, inorganic salts, and other substances. On a macroscopic scale, variations in wood structure manifest in the tree's morphology, overall dimensions, and material characteristics such as density, weight, thermal conductivity, and strength. On a microscopic level, alterations in wood volume and mechanical attributes can largely be ascribed to the interconnected, meticulously arranged, vertically oriented network of pores established by cells during the tree's growth process.[54] Trees possess an energy-water system which is biologically based encompassing together softwood and hardwood varieties, distinguished by their notable hydrophilic nature, intricate network of interconnected pores, diminished thermal conductivity, and varied mechanical characteristics.[55] Wood exhibits a notable abundance of vertically aligned microchannels within its tracheid, fibers, and vessels, boasting diameters ranging from 20 to 140 μm, which facilitate the transportation of ions, water, and essential nutrients (as depicted in Figure 3(a). From a chemical perspective, the wood cell wall is comprised of a complex matrix, consisting of cellulose (constituting 40–45% of its weight), hemicellulose (accounting for 20–35% of its weight), and lignin (making up 10–30% of its weight), as illustrated in Figure 3(b). This intricate composition underscores the wood's remarkable structural and functional properties.[56] Cellulose and hemicellulose, polysaccharides prevalent in natural biomass, exhibit the capacity for controlled carbonization, with cellulose standing as a biopolymer which is found abundantly on Earth.[56,57] From the molecular perspective, cellulose is made up of β-1–4 which is linked with D-glucose $(C_6H_{10}O_5)_n$ chain constituted of repetitive units of glucose by covalent bond as well as hydrogen bond.[58–60] Due to variations in species and geographic origins, different wood types exhibit diverse microstructural compositions. Firstly, in softwoods, tracheid's, commonly known as fiber cells, measure between 30 and 45 μm in tangential diameter and 3–5 mm in length, contrasting with the typically shorter vessels, ranging from 0.75 to 1 mm in length. Secondly, examining hardwoods, vessels display lengths ranging from 350 to 800 μm and diameters spanning 100–200 μm, while fibers in hardwoods, though generally shorter in length and smaller in diameter compared to softwoods, exhibit mean dimensions ranging from 0.5 to 2 mm in length and 10–50 μm in diameter. Both hardwood and softwood cells feature pits connecting adjacent cells.[61]

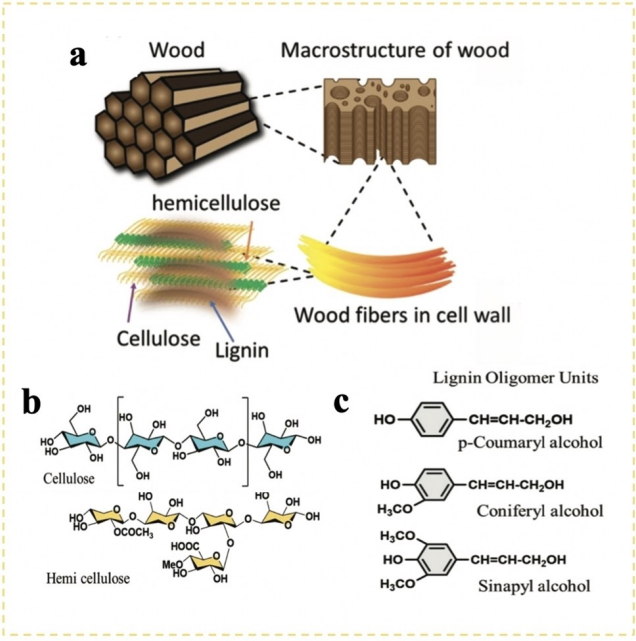

Figure 3. a) Diagram of the macro structure and constituents of wood. b) Cellulose, hemicellulose, and lignin (the three primary components of wood) molecular structures. c) Three different alcohol monomers of lignin. Adapted from Ref.[56] Copyright (2024) with permission from Wiley-VCH GmbH.

In essence, softwoods consist of a limited array of cell types characterized by uniform arrangement and simplistic pore structures, whereas hardwoods comprise a diverse array of cell types with intricate development. Consequently, hardwoods are perceived to exhibit more discernible multi-tiered pore architectures, encompassing macroscopic, mesoscopic, microscopic, and nanoscopic pores.[62] Softwood exhibits a relatively simplistic and homogeneous architecture, distinguished by a profusion of fibers arranged in a neat and organized manner.[56,63] In contrast, hardwood exhibits a more intricate and structure, marked by an abundance of vessels and increased density, thereby distinguishing itself from softwood.[58] In actuality, the inherent porosity within timber typically exhibits a hierarchical organization across four distinct orders of magnitude: nanostructures ranging from 0.1 nm to 10 nm, ultrastructure's spanning from 1 nm to 1 μm, microstructures ranging from 1 μm to 0.1 mm, and macrostructures extending from 0.1 mm to 10 cm.[64] Porosity and anisotropy are inherent attributes of wood, contributing to its distinctive characteristics. For lithium-ion batteries (LIBs), both hardwood and softwood can be used as precursors for carbon materials in the anode.[65] Hardwood-derived carbon tends to have a higher density and greater structural complexity, potentially leading to improved specific capacity. The porosity and interconnectedness of the carbon structure also play a significant role in battery performance.[66] Similarly, in sodium-ion batteries (SIBs), the differences in cellular structure between hardwood and softwood can influence their performance. The intricate cellular structure of hardwood may provide better pathways for sodium-ion diffusion, potentially resulting in enhanced performance compared to softwood. The specific performance differences may vary based on the specific characteristics of the wood-derived carbons and the electrode design.[67]

While scholars engage in ongoing discourse regarding the supramolecular configuration of cellulose, there is a prevailing consensus regarding the organization of cellulose chains within crystalline domains. The fundamental fibril structure longitudi-

nally encompasses numerous crystalline and amorphous segments. Cellulose is observed to represent such attributes of integral strength and rigidity stemming from both intra as well as intermolecular interactions.[68] Nanocellulose fibers, boasting diameters ranging from 5 to 20 nanometers, can be isolated from bundles of cellulose with diameters spanning over tens of nanometers.[69] Since the 1980s, various methods have been employed to extract nanocellulose fibers from plant cell walls, algae, and other organisms, encompassing top-down approaches. These include mechanical homogenization, as well as techniques like solvent dissolution and bacterial synthesis of bacterial cellulose. These diverse techniques have enabled the effective separation and harnessing of nanocellulose fibers, unlocking their vast potential for various applications.[70,71] Based on their raw constituents and morphological attributes, nanocellulose fibers are typically categorized into three classifications: cellulose nanocrystals (CNCs), nanofibrilled cellulose (CNFs), and bacterial cellulose (BCs). Nano-cellulose emerges as a prime candidate for fabricating diverse derivative carbon electrodes, owing to its elevated aspect ratio, substantial carbon content, plentiful active sites, and amenability to modification. These attributes facilitate the creation of electrodes characterized by heightened surface area, customizable pore microstructures, and doped compositions.[72,73] Lignin, a heterogeneous and amorphous polymer, constitutes a substantial portion of the cellular framework within wood. It is the second most abundant biopolymer globally, trailing only cellulose in prevalence.[74,75] There are various categories of cinnamyl alcohol by which Lignin is made up of. These include p-coumaryl, coniferyl and sinapyl alcohol Figure 3(c).[56] Lignin is classified into three primary categories such as p-hydroxyphenyl (H), eugenol (G), and guaiacol (G). These are categorized by variations in the position and quantity of methoxy groups on the phenolic nucleus. Hence there is a heterogeneous distribution of monomeric constituents across diverse wood species. Notably, softwood lignin is largely made up of G units, on the other hand hardwood lignin encompasses together G and S units, highlighting the diverse array of commercial lignin variants. These include soda lignin, organosolv lignin, kraft lignin, and lignin sulfonates. These variants present opportunities for innovative investigations and applications in the realm of secondary batteries.[76] Lignin stands out as the premier precursor for lithium-ion and sodium-ion batteries among the components of wood. Its unique properties render it an exceptional choice for producing electrode materials vital to these battery types. Lignin's substantial carbon content makes it an ideal candidate for generating carbon-based electrode materials, crucial for efficiently storing and releasing ions during charge and discharge cycles in Li-ion and Na-ion batteries.[77] Likewise, lignin's derivation from wood underscores its status as a renewable and abundant resource, offering a sustainable solution for energy storage applications. Its consistent availability ensures a reliable and environmentally friendly source for the large-scale production of battery materials. The intrinsic structural stability of lignin, owing to its extensively cross-linked composition, augments its mechanical robustness and thermal endurance. These attributes are indispensable for electrode materials, ensuring the structural integrity of electrodes during the charge-discharge process.[78] Additionally, lignin-derived carbon materials offer versatility through tunable properties, allowing customization of specific surface area, pore size distribution, and electrical conductivity. This adaptability enables the optimization of electrode materials to meet the precise requirements of Li-ion and Na-ion batteries. Hence, lignin's high carbon content, renewable nature, structural stability, tunable properties, and environmental benefits collectively position it as the optimal precursor for Li-ion and Na-ion batteries sourced from wood.[79]

Wood contents can be converted into carbonaceous materials through pyrolysis, a process in which the wood is heated in the absence of oxygen. This thermal decomposition transforms the complex organic structures present in wood into carbon-rich residues. By carefully controlling the pyrolysis conditions such as temperature, heating rate, and residence time the properties of the resulting carbon products can be tailored to meet specific requirements for various applications. Additionally, the presence of heteroatoms such as oxygen, nitrogen, and phosphorus in wood can lead to the formation of functional groups on the surface of the carbonaceous material during pyrolysis. These functional groups can improve the electrochemical performance by enhancing the wettability of the electrolyte and providing additional active sites for ion storage. The graphitization degree of the carbon material, which can be manipulated by adjusting the pyrolysis temperature, plays a crucial role in determining the electrical conductivity and structural stability of the anode. Using wood-derived carbonaceous materials as anodes in Li-ion and Na-ion batteries not only leverages the renewable and abundant nature of biomass resources but also contributes to sustainability and environmental friendliness. Beyond energy storage, wood-derived carbonaceous materials have versatile applications in fields such as catalysis, gas storage, water purification, and sensor technology. These materials can offer competitive performance compared to traditional graphite anodes, with the potential for higher capacity, improved rate capability, and better cycling stability.[80]

4. Attributes and Significance of Wood-Derived Materials in LIBs and SIBs

Numerous carbon allotropes and textures, including graphite (Gr), carbon nanotubes (CNT), and graphene, have demonstrated remarkable electrochemical reversibility. However, their widespread adoption is impeded by the intricate and costly synthesis methods which limits their potential applications. The convoluted synthesis processes and prohibitive production costs pose significant obstacles to their widespread utilization.[81,82] Henceforth, the synthesis of carbon-based materials sourced from sustainable reservoirs such as biomass has garnered significant attention. Fabrication of biomass into porous materials with functional groups, renders their eminent suitability for battery applications. Carbon materials derived

from biomass precursors exhibit a spectrum of desirable traits, including substantial specific surface area (SSA), diverse pore architectures encompassing micro and mesopores, a profusion of surface functional groups, adjustable hydrophilicity, and heightened conductivity. Leveraging these attributes, such materials find successful application as anode materials in both lithium-ion batteries (LIBs) and sodium-ion batteries (SIBs).[14]

In addition, creating wood-derived carbon electrodes for Li/Na-ion batteries involves a specific process that capitalizes on the natural structure of wood to produce high-performance carbon electrodes. The process typically includes several key steps. First, an appropriate type of wood, such as pine, poplar, or eucalyptus, is selected due to its natural porosity, high cellulose/lignin content, and favorable carbonization properties. The selected wood then undergoes pre-treatment to remove impurities, extractives, and moisture, which may involve washing, drying, and potential chemical treatment to enhance its suitability for carbonization. The pre-treated wood is then subjected to controlled carbonization under high temperatures in an inert atmosphere, such as nitrogen or argon. This process thermally decomposes the wood components and transforms them into carbon while preserving the natural porous structure of the wood. In some cases, the carbonized wood may undergo an activation process to further enhance its porosity and surface area. This can be achieved through physical methods like steam activation or chemical methods using activating agents like KOH or $ZnCl_2$. Following carbonization and possibly activation, the resulting wood-derived carbon material may undergo post-treatment processes to modify its surface chemistry, optimize its pore structure, and improve its electrochemical properties. Treatments with acids, bases, or other chemicals may be employed to tailor the material for specific battery applications. Finally, the processed wood-derived carbon material is used to fabricate the electrodes for Li/Na-ion batteries. This involves mixing the carbon material with binders and conductive additives, pressing it onto current collectors, and shaping it into the desired electrode architecture. The inherent porosity, carbon content, and natural structure of wood make it an attractive precursor for producing carbon materials with excellent electrochemical properties, for sustainable energy storage technology.[83–85]

4.1. Constructed Defects and Nanochannels

The naturally occurring hierarchical porosity of wood endows electrodes with unique structural functionalities. Macropores function as efficacious repositories for the transit and retention of electrolyte ions, substantially improving their diffusion rates as well as their kinetic properties. The mesoporous structure facilitates ion exchange within the electrode, thereby optimizing performance metrics under high current densities. The micropores serve as conduits for ion immersion within electrolytes, a crucial aspect for enabling high-energy storage capabilities, thereby underscoring the synergistic role of hierarchical porosity in augmenting electrode performance.[86] It has been observed that under different carbonization temperatures and chemical treatments wood pore size varies.[87] The surface area of natural wood typically ranges from 1–50 m^2/g.[88] The pore distribution of wood encompasses a wide range of pores such as micropores (less than 2 nm), mesopores (ranging from 2 nm to 50 nm) and macropores (having diameter greater than 50 nm).[89] It's pertinent to note that providing a specific numerical range for the tortuosity of natural wood is challenging due to the complex and heterogeneous nature of wood structures. It can vary significantly based on factors such as wood species, growth conditions, age, and processing methods. Additionally, tortuosity is often influenced by the scale at which it is measured (e.g., at the microscale within individual cells or at the macroscale within the overall wood structure).[90]

In addition, Subsequent to the carbonization process, wood-derived carbon characteristically exhibits a macroscopic structure defined by open and well-aligned channels, featuring a scale that spans meters, thereby yielding a hierarchical architecture that is conducive to optimal mass transport and electrochemical reactivity. The resultant carbon material displays a unique morphology, distinguished by its expansive and ordered channel network, which arises from the preservation of the natural wood structure during carbonization.[91] Vertical channels within wood provide an efficacious buffer zone for the transit and retention of electrolyte ions, thus markedly augmenting the rate of diffusion and reaction kinetics. Mesopores play a pivotal role in optimizing performance rates, particularly under elevated current densities, by facilitating dynamic ion exchange within the electrode. Micropores facilitate the immersion of ions within electrolytes, constituting a crucial component in achieving efficient and effective high-energy storage capabilities.[56] There can be a connection between the channel structure and electrode materials derived from wood. The hierarchical and porous structure of wood can provide unique advantages for electrode materials, including high surface area, good mechanical properties, potential for high energy and power density. The channel structure of wood, which consists of interconnected vascular bundles for water and nutrient transport, can serve as a template for creating porous electrode materials with interconnected channels for ion transport.[92,93] By removing lignin and hemicellulose from wood through processes such as carbonization or activation, a porous structure can be obtained that is suitable for accommodating electrochemically active materials. In addition, carbonized or activated wood-derived materials can provide a sustainable and renewable alternative to traditional carbon-based electrode materials for energy storage technologies.[94] Hence, the channel structure of wood can influence the design and characteristics of electrode materials derived from wood, offering unique opportunities for the development of sustainable energy storage devices.

4.2. Low-Tortuosity Channels

Porous architectures characterized by aligned structures reminiscent of wood exhibiting low tortuosity in a singular direction or open structures akin to sponge-like microstructures (display-

ing less tortuosity uniformly in all directions) are sought-after to augment electrode thickness without compromising power density as well as equipment efficacy.[95] Tortuosity is proportional to the ratio of the actual ion diffusion distance and the electrode thickness.[96] The minimum tortuosity having value equal to 1 occurs in which ions traverse straight channels aligned in a parallel direction during diffusion. Decreasing the tortuosity of the electrode facilitates charge transport kinetics, thereby amplifying the performance of the battery.[97] The incorporation of readily reachable channels, coupled with flexible thickness ranging between (5–30 μm) while extending to hundreds of μm, engenders a customized electrode framework for prolonged cycling.[98] It has been observed that electrodes possessing low tortuosity tends to exhibit quicker lithium-ion transfer, and low concentration polarization.[99] The attainment of such minimal tortuosity is feasible through wood-nanoarchitecture, distinguished by its distinctive surface structure. Tortuosity factors have been employed to discern the ion/electron transport impediments in batteries, wherein ions navigate through convoluted pathways, facilitating the identification of the genuine bottleneck in charge transport.[100] Hence, an anode crafted from wood exhibiting a micro-nanopore configuration proves advantageous for accommodating elevated quantities of active materials, facilitating ion transport. Such low-tortuosity materials, typically deemed unsuitable for fabricating high-energy density devices, become viable options.[56]

4.3. Mechanical Strength of Wood Assemblies

With effective energy storage and conversion, materials obtained from wood present a fitting choice, owing to their manifold advantages. These encompass hierarchically porous structures, exceptional mechanical flexibility, integrity, and versatile multifunctionality. Wood-based assemblies exhibit remarkable resilience, enduring considerable weight loads, and demonstrate notable recovery from compression, as depicted in Figure 4(a).[56] The exceptional mechanical strength of wood based carbon (WC) is attributable to its inherent abundance of aligned channels, which persists even after undergoing high temperature carbonization and also post treatment as depicted in Figure 4(b). The quest for enhanced electrochemical performance and mechanical properties in wood-based materials is required for high flexibility, toughness, and strength. Delignification approach offers an innovative solution, circumventing the need for thermal treatment at relatively higher temperature, rendering wood electrically conductive while preserving its mechanical toughness and flexibility.[101] The incorporation of polymers provides elevated conductive and mechanical properties to the porous architectures.[102]

In conclusion, biomass-derived carbon materials, which can be easily modified, have emerged as promising successors for high-energy density anode candidates in both lithium-ion batteries (LIBs) and sodium-ion batteries (SIBs). To tailor the properties of biomass carbon anodes to meet the demands of LIBs and SIBs, a thorough evaluation of the synergistic effects resulting from the combination of various factors during carbon material synthesis is necessary. This requires a comprehensive understanding and integration of strategies involving pyrolysis, activation, and heteroatom doping. These processes can help to attain an ideal balance among the crucial physical, chemical and electrochemical parameters essential for realizing high energy and power density in biomass carbon anodes. By getting the potential of biomass-derived carbon materials, significant advancements can be made in the development of sustainable and energy solutions with high performance.[103]

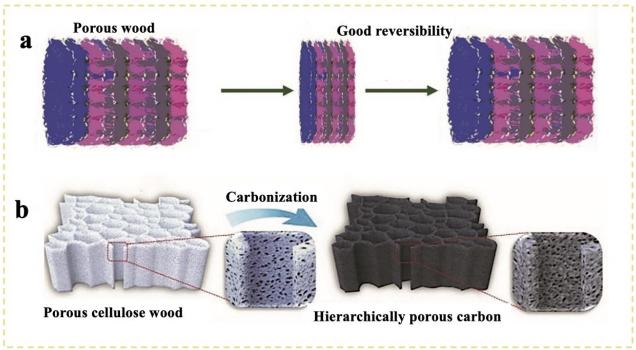

Figure 4. a) Stability of wood. b) Synthesis procedure of porous carbon thick electrode derived from wood. Adapted from Ref.[56] Copyright (2024) with permission from Wiley VCH GmbH.

5. Wood-Structured Anodes for LIBs

The utilization of wood-structured anodes for LIBs delves into the burgeoning field of sustainable energy storage, spotlighting the promising integration of wood-derived materials in lithium-ion battery (LIB) technology. This approach capitalizes on wood's intricate hierarchical architecture, characterized by abundant micropores and anisotropic structure, to address critical challenges facing LIBs. By leveraging the unique properties of wood, such as its high surface area-to-volume ratio and mechanical robustness, researchers aim to pioneer a new generation of LIB anodes with enhanced performance, longevity, and environmental sustainability. In lithium ion batteries (LIBs), the typical components are anode, which is made of graphite or carbon, an organic electrolyte which contains lithium salt as a source of Li^+ ions and cathode which is made of a transition metal oxide.[104–107] For high-performance lithium-ion batteries (LIBs), it is imperative to engineer superior carbon (anode) materials possessing attributes such as high electrical conductivity, moderate surface area, optimal porous structure, and substantial heteroatom doping, all while maintaining cost-effectiveness.[108–110] Overall, numerous types of wood derived anode materials have been utilized so far to enhance the electrochemical performance of LIBs as shown in Table 2.

Table 2. Synthesis process and performance of various wood used in LIBs.

Wood species	Synthesis procedure	Electrochemical performance	Ref.
Mangrove charcoal	Carbonized at 700–1300 °C in Ar atmosphere	335 mAh/g at 0.1 C after 50 cycles	[113]
Mangrove green tree	Carbonized at 800 °C in Ar atmosphere	424 mAh/g at 30 mA/g after 100 cycles	[114]
Loblolly pine trees	Pyrolyzed at 850 °C in N_2 atmosphere	1000 mAh/g at 0.1 C after 250 cycles	[115]
Wood fiber	Carbonized at 600 °C in N_2 atmosphere	952 mAh/g at 0.1 A/g after 100 cycles	[116]
Softwood pulp derived NFC	Carbonized at 1000 °C in 95 % Ar/5 % H_2	312 mAh/g at 25 mA/g after 63 cycles	[117]
Balsa Wood	Pyrolysis at 1100 °C in N_2 atmosphere	300 mAh/g at 0.1 C after 400 cycles	[118]
Pine wood	Carbonized at 1000 °C in Ar atmosphere	734 mAh/g at 200 mA/g after 100 cycles	[119]
C-SnOx wood fibers	Carbonized at 1000 °C in 95 % Ar/5 % O_2	280 mAh/g at 1000 mA/g after 100 cycles	[120]
SnO_2/WFPC nanodots wood flour	Carbonized at 600 °C in Ar atmosphere	1014.4 mAh/g at 156 mA/g after 100 cycles	[121]
Porous Carbon Framework (PCF/Si)	Carbonized at 650 °C in Ar atmosphere	891 mAh/g at 200 mA/g after 400 cycles	[122]
Wood pulp fiber SiO_2/C composite	Carbonized at 600 °C in Ar atmosphere	1130 mAh/g at 100 mA/g after 200 cycles	[123]
Pinewood (LCO)	Carbonized at 700 °C in Air atmosphere	64 mAh/g at 0.5 C after 30 cycles	[124]
Softwood pulp (CNF-CB/LFP)	TEMPO-oxidation treatment	121 mAh/g (90 %) at 2 mA/cm^2 and 20 mg/cm^2	[125]

5.1. Pristine-Wood Based Anodes

Pristine wood-based anodes have emerged as favorable candidates for enhancing the performance and sustainability of lithium-ion batteries (LIBs). With growing concerns over environmental impact and resource depletion associated with traditional graphite-based anodes, the exploration of renewable and abundant materials like wood offers a compelling avenue for advancing battery technology. Pristine wood, with its inherent hierarchical structure and abundance in nature, presents unique opportunities for addressing the challenges of energy storage. This section explores the utilization of pristine wood as anodes in LIBs, highlighting their structural characteristics, electrochemical properties, and potential applications in next-generation energy storage devices. Wang et al., systematically explored the performance of hard carbon electrodes made of wood pre-cursor.[111] Balsa wood, poplar wood, and birch wood were meticulously chosen to conduct a systematic investigation into their roles as precursors in shaping the structure and lithium-storage capabilities of wood-based hard carbon thick electrodes (WHCTEs). Bal-W exhibits a profusion of mesopores ranging from 2 to 4 nm, while Pop-W displays a moderate quantity of mesopores. In contrast, Bir-W manifests a scarcity of mesopores but boasts abundant micropores concentrated at 1.2 and 1.6 nm, as illustrated in Figure 5(a). During battery testing, owing to its highest mass loading, Bir-W showcased the most substantial residual capacity among the three samples after 200 cycles at 1 mA/cm^2. The residual capacities of Bir-W, Pop-W, and Bal-W stood at 12.27, 34.15, and 41.03 Ah/L, respectively. It is discerned that mass loading, specific surface area, and pore size distribution wield significant influence over electrode capacity performance and the kinetic attributes governing the storage of lithium ions within WHCTEs furnish valuable insights for the realm of alkali metal ion batteries utilizing such materials. Drews et al., employed biomass derived hard carbon anodes in combination with an in-situ electrochemical pre-lithiation process for lithium-ion full-cells Figure 5(b).[112] Exhibiting notable capacities, exceptional rate capability, and impressive capacity retention, spruce hard carbon emerged as a compelling contender for supplanting conventional graphite in lithium-ion battery (LIB) anodes demonstrating a noteworthy discharge capacity of 300 mAh/g, accompanied by a compact anode surface, as illustrated in Figure 5(c and d). Despite the promising attributes of pristine wood-based anodes for lithium-ion batteries (LIBs), several challenges and drawbacks must be addressed to realize their

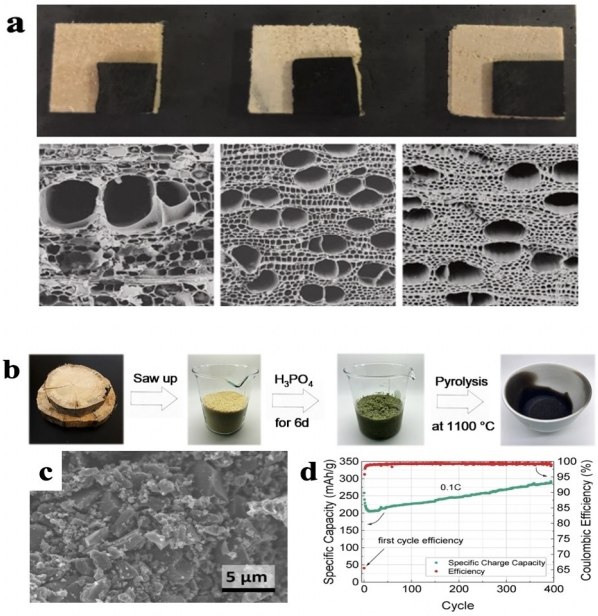

Figure 5. a) Before and after carbonization of carbon electrodes derived from wood (from left to right: Bal-W, POP–M, Bir-W) and top to bottom morphological results of these wood-based carbon electrodes corresponding to Bal-W, Pop-W, and Bir-W. Adapted from Ref.[111] Copyright (2023) with permission from Elsevier. b) Diagram of spruce hard carbon synthesis. c) SEM of spruce hard carbon anode. d) long-term cycling of spruce hard carbon anode. Adapted from Ref.[112] Copyright (2021) with permission from Wiley-VCH GmbH.

full potential. One significant issue is the lack of uniformity and consistency in the structure and composition of natural wood, leading to variations in performance and stability among different samples. Additionally, the high porosity and complex microstructure of wood can hinder the efficient diffusion and storage of lithium ions, resulting in lower energy density and cycling stability compared to conventional graphite anodes. The susceptibility of wood to mechanical degradation, such as swelling, shrinking, and dendrite formation during charge-discharge cycles, poses durability concerns that may limit the long-term reliability of wood-based LIBs. Addressing these challenges will be crucial for realizing the full potential of pristine wood-based anodes and integrating them into practical LIB applications.

Wu et al. innovatively devised a novel methodology to craft Fe_2O_3@C, leveraging peanut-derived woody material via a meticulous two-step hydrothermal process followed by low-temperature calcination, aided by $Fe(NO_3)_3$ as depicted in Figure 6(a).[127] Functioning as an anode for lithium-ion batteries (LIBs), the Fe_2O_3@C composite demonstrated exemplary electrochemical prowess, manifesting a specific capacity of 1000.8 mAh/g at 200 mA/g post 100 cycles. This notable enhancement can be attributed to the synergistic interplay between the porous carbon matrix and the embedded Fe_2O_3 nanoparticles. This amalgamation facilitated an augmented contact interface between the electrolyte and the active constituents, concurrently bolstering conductivity while adeptly accommodating volumetric fluctuations via the provision of supplementary void space during the cyclic operation. This seminal endeavor holds promise in furnishing a transformative pathway towards ameliorating anode materials, thereby ushering in a new era characterized by heightened reversible capacity as shown in Figure 6(b). Huang et al. undertook the fabrication of composites comprising Manganese oxide loaded with wood based carbon fibers (CF@MnO) using a straightforward as well as ecologically sustainable approach.[126] This method led to a reduction in specific surface area, attributable to the formation of MnO nanoparticles on the carbon fibers. Scanning electron microscopy (SEM) images, depicted in Figure 6(c and d) elucidate the structural distinctions between the anode configurations with and without MnO nanoparticles. The CF@MnO composites showcased outstanding electrochemical performance as anode (LIBs), manifesting high reversible capacities within the range of 530–726 mAh/g at a current density of 100 mA/g. The optimized CF@MnO variant, with a MnO-to-carbon ratio of 1 : 2, demonstrated a reversible capacity of 734 mAh/g and 265.3 mAh/g at current densities of 100 mA/g and 2000 mA/g, respectively. Additionally, the material exhibited exceptional stability, maintaining a coulombic efficiency of approximately 100 % after 200 cycles at a high current density of 400 mA/g (Figure 6e and f), alongside notable rate capability, as evidenced by significant outcomes, thus underscoring its potential as an ideal candidate for high-performance LIB anode materials.

Revathi et al. explored C–SnO_x composites obtained from wood fibers as LIB anode.[128] The templating process of fibers derived from wood through impregnation with tin isopropoxide acetyl acetone served a dual function. Firstly, it effectively postponed the hydrolysis of tin isopropoxide, while concurrently stabilizing the structural integrity of the wood fibers and preserving their porosity throughout the carbonization process. Secondly, the incorporation of oxygen (5 %) during the process of carbonization facilitated the passivation of metallic tin nanoparticles, resulting in the uniform dispersion of SnO_x nanoparticles within the carbon matrix, as depicted in Figure 7(a). The amalgamation of a carbon matrix possessing porous structure with a blend of Sn, SnO, and SnO_2 in CO-SnO_x@1000 °C stands as the primary factor contributing to the superior and enduring capacity, alongside maintaining a stable anode structure. In rate capability investigations, initiated with a current density of 1 A/g, remarkably stable high capacities in

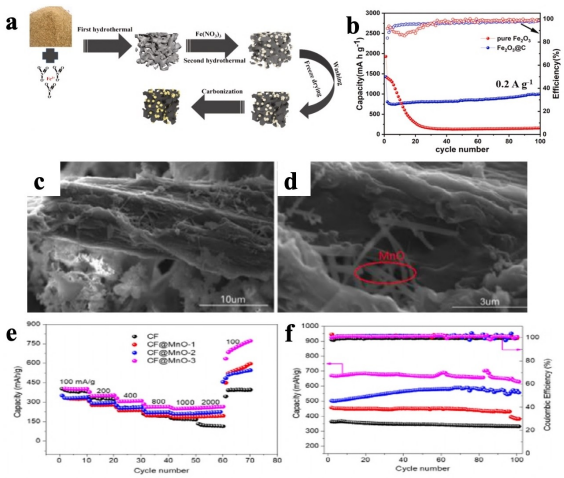

Figure 6. a) Synthesis procedure of Fe_2O_3@C. b) The cycling performance of the material was evaluated at 1 C for 200 cycles, with an inset displaying transverse sections of pine wood-derived activated carbon (AC). Adapted from Ref.[127] Copyright (2023) with permission from Elsevier. c,d) SEM images of CF@MnO-3 (e) charge discharge rate performances at various current densities. f) Cycling stability at 100 mA/g for various CF@MnO samples (black, red, blue, magenta represent CF, CF@MnO-1, CF@MnO-2, CF@MnO-3 respectively. Adapted from Ref.[126] Copyright (2022) with permission from Elsevier.

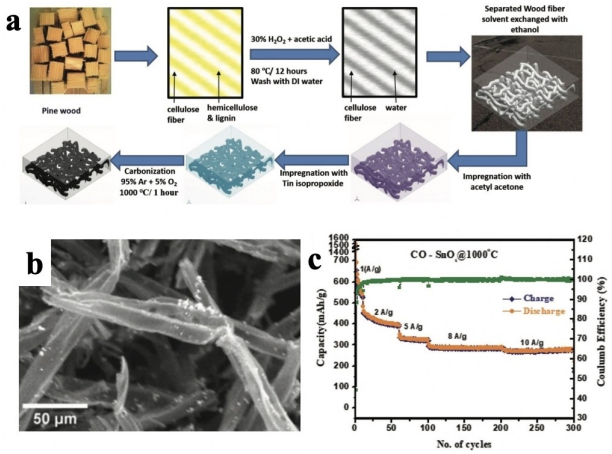

Figure 7. a) Schematic synthesis for C-SnO_2 composite. b) C-SnO_x@1000 °C. c) cycling stability and rate capability of CO-SnO_x@1000 °C at 1 A/g. Adapted from Ref.[128] Copyright (2020) with permission from Wiley-VCH GmbH & Co.

the range of 260–280 mAh/g, accompanied by exceptional Coulombic efficiency as well as cycle stability over 100 cycles, were achieved at elevated current densities of 8 A/g and 10 A/g, correspondingly, as illustrated in Figure 7(b and c). This composite material derived from pine wood-based carbon and SnO_x demonstrates its mettle as a highly promising candidate for anode material applications.

In addition, Zhang et al., incorporated SnO_2 nanodots in wood floor-derived porous carbon and synthesized them employing a hydrothermal technique in combination with carbonization treatment Figure 8(a).[129] The anode materials under scrutiny exhibited the integration of SnO_2 onto their surfaces, as evidenced in Figure 8(b). The synthesized SnO_2/WFPC composites as anode for LIB demonstrated an impressive initial reversible capacity of 1014.4 mAh/g at 156 mA/g. This enhanced electrochemical performance can be credited to the nanoconfined nature of SnO_2 particles embedded within porous conductive carbon, facilitating a reduction in the diffusion length of Li^+ ions, promoting facile electrolyte access, and ensuring robust mechanical integrity Figure 8(c). The microfibrils found within the fibers of wood pulp constituting the cell wall of plant exhibit an inherently orderly and intertwined configuration, imparting a structurally stable porous framework. These fibers possess exceptional mechanical resilience and facilitate conductivity, particularly beneficial for silicon-based materials. Leveraging these advantageous properties. When applied in lithium-ion batteries (LIBs), wood-metal oxide composite anodes encounter various challenges and limitations. The incorporation of wood with metal oxides is hampered by factors such as inconsistent performance stemming from variations in wood structure, restricted ion diffusion and storage due to the high porosity and intricate microstructure of wood, and mechanical degradation over cycling. Overcoming these hurdles is essential to unlock the complete potential of wood-metal oxide composite anodes for practical lithium-ion battery (LIBs) applications.

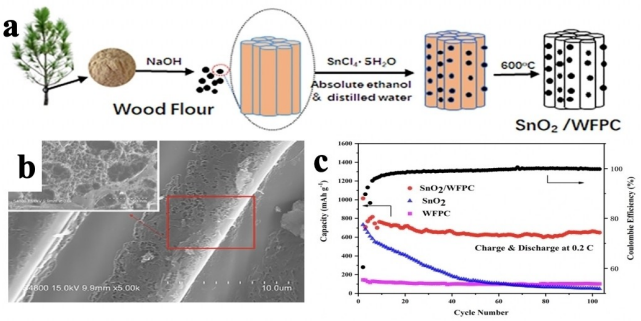

Figure 8. a) Synthesis route for SnO_2/WFPC composite. b) SEM images of wood flour-derived porous carbon. c) Cycling performance of various samples at 0.2 C. Adapted from Ref.[129] Copyright (2020) with permission from Elsevier.

5.2. Wood-Si/SiO_2 Composite Anodes

Wood-Si and SiO_2 composite anodes present an auspicious pathway to bolster the efficacy and capacity of lithium-ion batteries (LIBs). By amalgamating wood-derived carbon matrices with silicon (Si) and silicon dioxide (SiO_2), these composite materials exhibit distinctive merits in energy storage applications. The integration of Si and SiO_2 into the carbon framework derived from wood yields synergistic effects, thereby increasing the electrochemical performance and stability of the anode. In a study, He et al. achieved a breakthrough by crafting a porous carbon framework (PCF) as an anode material through a pore-forming technique employing K_2FeO_4, coupled with surface functionalization utilizing a mixed acid derived from natural grape woody stems Figure 9(a).[130] Characterized by a uniform distribution of through-holes with copious micropores adorning the carbonaceous walls, the PCF matrix served as an ideal substrate for the encapsulation of silicon nanoparticles (Si NPs), yielding PCF/Si composite architectures Figure 9(b). The abundant oxygen-functional groups inherent within the matrix facilitated the immobilization of Si NPs within the internal through-holes, thereby bestowing upon them exemplary electron conductivity properties while adeptly mitigating the volumetric expansion associated with silicon. Consequently, the PCF/Si composite emerged as a frontrunner, showcasing an unprecedented specific capacity of 642 mAh/g post 200 opera-

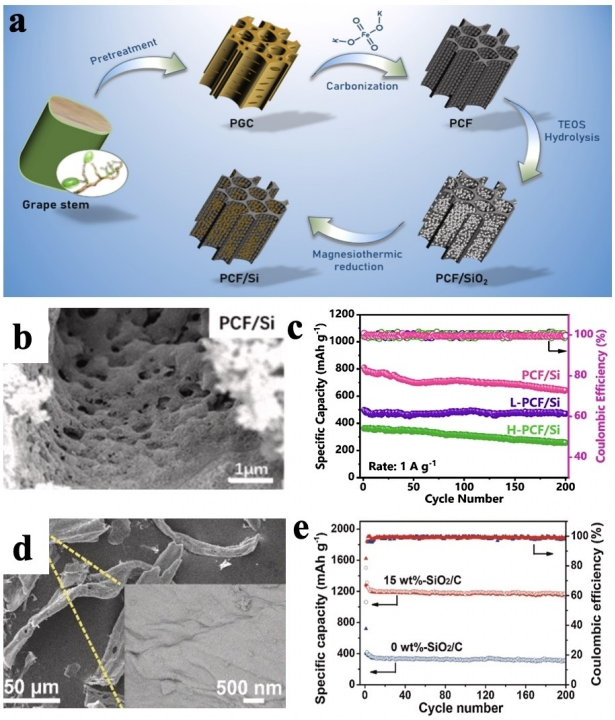

Figure 9. a) Synthesis procedure of the PCF/Si composites. b) Scanning Electron Microscopy (SEM) image of PCF/Si. c) cycling performance of the PCF/Si, L-PCF/Si and H-PCF/Si composites at 1 A/g. Adapted from Ref.[130] Copyright (2022) with permission from Elsevier. d) SEM images of SiO2/C composite for 0 wt%-SiO_2/C. e) cycling performance of 0 wt%-SiO_2/C and 15 wt%-SiO_2/C composites at 100 mA/g. Adapted from Ref.[131] Copyright (2020) with permission from Elsevier.

tional cycles, correlating to an impressive capacity retention rate of approximately 79.4% and a nominal decay rate of merely 0.1% foe every cycle. Residual capacities observed for the L-PCF/Si and H-PCF/Si variants stood at 471 mAh/g and 257 mAh/g, correspondingly. This seminal investigation unveiled a pioneering methodology leveraging wood-derived carbon as a carrier for silicon, thereby laying a solid foundation for the widespread adoption of Si/C composite anodes in practical energy storage applications as delineated in Figure 9(c). Wang et al. proposed a methodology harnessing wood pulp fibers in the fabrication of SiO_2/C composites.[131] In this study, the alkali pretreatment was employed to disrupt the hydrogen bonds within the wood pulp fibers, leading to an expansion of the spatial distance between cellulose microfibrils and exposing a greater surface area. This facilitated a more uniform embedding of SiO_2 throughout the carbon skeleton during the subsequent carbonization process. Consequently, the resulting SiO_2/C composite exhibited a highly mesoporous structure with a tubular morphology, as depicted in Figure 9(d). Additionally, remarkable electrochemical performance was observed. A high columbic efficiency of around 84.9% was achieved, while a reversible specific capacity of 1130 mAh/g was attained maintaining a coulombic efficiency of 98.8% after 200 cycles at 0.1 A/g, as illustrated in Figure 9(e).

Wood-Si/SiO_2 composite anodes for LIBs face several challenges and drawbacks, including issues related to volume expansion and contraction during lithiation and delithiation cycles, leading to mechanical degradation and eventual pulverization of the electrode material. The high surface area of silicon and silicon dioxide can also result in increased reactivity with the electrolyte, leading to the creation of SEI layer that hampers ion transport and decreases cycling stability. Additionally, the synthesis of wood-Si/SiO_2 composites often involves complex and costly procedures, limiting their scalability and commercial viability. Achieving uniform distribution and strong adhesion of silicon and silicon dioxide within the wood-derived carbon matrix remains a significant challenge. It affects the overall electrochemical performance and durability of the anode. Addressing these challenges is crucial for realizing the full potential of wood-Si/SiO_2 composite anodes in LIBs and advancing their practical application in next-generation energy storage devices. In conclusion, the integration of wood-structured anodes presents a promising avenue for advancing lithium-ion battery (LIB) technology towards sustainability and enhanced performance. We have demonstrated the feasibility and potential benefits of utilizing wood-derived materials in LIBs, including improved capacity retention, cycling stability, and mechanical flexibility. However, several challenges remain to be addressed. These include optimizing the synthesis and processing techniques to ensure uniformity and scalability of wood-based anodes, elucidating the underlying mechanisms governing the electrochemical performance of these materials, and addressing potential issues related to long-term stability and compatibility with existing battery components. Nevertheless, with concerted efforts, wood-structured anodes hold great promise for ushering in a new era of sustainable and high-performance energy storage solutions.

6. Wood-Structured Anodes for SIBs

The significance of wood structured anodes for SIBs reveals multiple approaches in the realm of energy storage, focusing on the utilization of wood-based materials as anodes for sodium-ion batteries (SIBs). Wood, renowned for its hierarchical structure and porosity, presents a compelling candidate for anode materials as a result of its abundant availability, low cost, and eco-friendliness. The unique characteristics of wood like its high surface area and natural channels helps to overcome the limitations encountered in traditional SIB anodes, including low energy density and poor cycling stability. By leveraging the inherent advantages of wood, innovative strategies for designing SIB anodes with enhanced electrochemical performance are paving the way for sustainable, highly economical and efficient solution for energy storage.[132] Overall, various wood derived anode materials have been used so far to enhance the electrochemical performance of SIBs as shown in Table 3.

6.1. Pristine-Wood Based Anodes

The utilization of pristine wood-based anodes for sodium-ion batteries (SIBs) presents a compelling avenue towards advancing the field of sustainable energy storage. Pristine wood, with its inherent hierarchical structure and abundant porosity, offers a promising substrate for accommodating sodium-ions during charge and discharge cycles. This unique architecture facilitates efficient ion diffusion and mitigates volume expansion issues commonly encountered with alternative anode materials. Xu et al. have strategically selected paulownia wood, characterized by its inherent porosity. Through annealing process they were able to yield carbon materials that exhibit exceptional electrochemical properties as depicted in Figure 10(a).[133] Upon SEM analysis, the anode material revealed a discernible structure and morphology characterized by well-defined channels and pores, as depicted in Figure 10(b). The resulting HC-1400

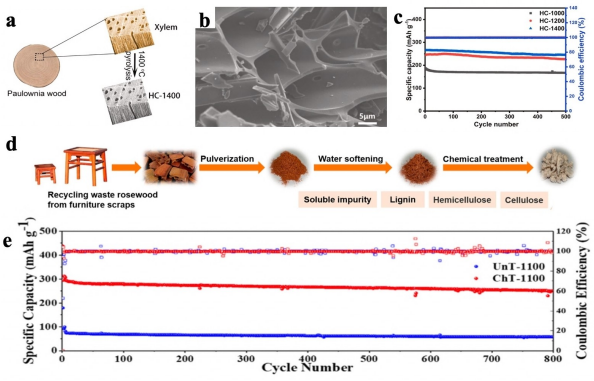

Figure 10. a) Synthesis route of the paulownia xylem hard carbon. b) HRTEM image of HC-1400. c) cycling performance at the current density of 1 C discharge and 5 C charge for 500 cycles. Adapted from Ref.[133] Copyright (2024) with permission from Elsevier. d) Schematic diagram of waste rosewood derived hard carbon. e) performance of BHCs at a current density of 500 mA/g. Adapted from Ref.[146] Copyright (2022) with permission from Wiley Online Library.

Table 3. Synthesis process and performance of various wood used in SIBs.

Wood species	Synthesis procedure	Electrochemical performance	Ref.
Natural fortune paulownia wood	Carbonized at 600 °C in Ar atmosphere	313 mAh/g at 0.1 C after 500 cycles	[134]
Waste wood rose derived hard carbon	Carbonized at 1100 °C in Ar atmosphere	326 mAh/g at 20 mA/g after 800 cycles	[135]
Camphor wood	Pyrolysis at 700 °C in Ar atmosphere	280 mAh/g at 2000 mA/g after 500 cycles	[136]
Basswood	Heat treated at 500 °C in N_2 atmosphere	326 mAh/g at 100 mA/g after 500 cycles	[137]
Pine wood	Pyrolysis at 500 °C in Ar atmosphere	354 mAh/g at 30 mA/g after 1000 cycles	[138]
Waste-wood	Carbonized at 1100 °C in Ar atmosphere	430 mAh/g at 50 mA/g after 50 cycles	[139]
Hardwood	Carbonized at 1000 °C in Ar atmosphere	75 mAh/g at 50 mA/g after 350 cycles	[140]
Monterey pine	Carbonized at 1000 °C in Ar atmosphere	126.1 mAh/g at 600 mA/g after 1000 cycles	[141]
Poplar wood	Pyrolysis at 1000 °C in Ar atmosphere	330 mAh/g at 2 C after 600 cycles	[142]
Natural wood fiber	Carbonized at 1000 °C in Ar atmosphere	196 mAh/g at 100 mA/g after 200 cycles	[143]
Balsa	Pyrolysis at (1000 °C, 1200 °C, and 1400 °C) in Ar atmosphere	439 mAh/g at 100 mA/g after 500 cycles	[144]
Porous wood fiber	Pyrolyzed at 900 °C in N_2 atmosphere.	266 mAh/g at 200 mA/g after 300 cycles	[145]

exhibited heightened graphitization and a reduced specific surface area (SSA), culminating in an impressive initial Coulombic efficiency of 85.9% and a reversible specific capacity of 313 mAh/g upon first charge/discharge, as illustrated in Figure 10(c). This investigation introduces a strategic approach for fabricating high-performance hard carbon negative electrodes utilizing a wood precursor. In another study, Zhou et al., successfully synthesized wood derived carbon with rich closed pores and thin pores from renewable rosewood by employing a chemical pretreatment method Figure 10(d).[146] Remarkably, this technique enables precise control over the formation of enclosed pores, resulting in a notable enhancement in electrochemical performance. Crucially, it achieves the creation of accessible enclosed pores at a comparatively lower carbonization temperature of 1100 °C, mitigating the hazards associated with high temperature processes and minimizing energy consumption. The specimen showcases remarkable sodium storage capabilities, boasting a commendable reversible capacity 326 mAh/g at 20 mA/g Figure 10(e). As evidenced, the substantial enhancement in sodium storage attributes of ChT-1100 can be primarily credited to the proliferation of plentiful and accessible enclosed pores with thinner pores. These pores not only afford ample space for sodium accommodation but also facilitate the diffusion of Na^+ within the bulk phase.

Pristine wood-based for sodium-ion batteries (SIBs) as anodes encounter several challenges and limitations. One significant concern is the comparatively lower specific capacity of wood-based materials when compared to conventional graphite or alloy-based anodes, potentially constraining the overall energy density of the battery system. The inherent variability in the properties of natural wood, including density, porosity, and moisture content, may lead to inconsistencies in electrochemical performance and cycling stability. Additionally, the incorporation of pristine wood into SIBs necessitates extensive pre-treatment procedures to eliminate impurities and enhance the material's electrochemical characteristics, increasing the complexity and cost of manufacturing. The structural degradation of wood-based anodes during prolonged cycling is attributed to mechanical stress and electrolyte infiltration, presenting a significant obstacle to achieve long-term durability and reliability in practical applications. Overcoming these hurdles is imperative to fully harnessing the

potential of pristine wood-based anodes for SIBs and promoting their integration into sustainable energy storage solutions.

6.2. Doped Wood-Based Anodes

The advent of doped wood-based anodes marks a significant stride in the realm of sodium-ion batteries (SIBs), offering a novel methodology to increase the electrochemical performance and stability of these energy storage devices. Through the strategic incorporation of dopant elements into the wood matrix, the properties of the anode material are tailored to address key challenges inherent in SIB technology. Doping introduces beneficial effects such as improved conductivity, enhanced specific capacity, and enhanced cycling stability, thereby mitigating issues related to sluggish kinetics, structural degradation, and limited capacity retention. In a study, Aristote et al. embarked on the fabrication of heteroatom-doped carbonaceous materials derived from camphor wood (Cmph), subsequently evaluating their electrochemical attributes as prospective anodes for sodium-ion batteries (SIBs) as depicted in Figure 11(a).[147] The scanning electron microscopy (SEM) imagery Figure 11(b) elucidated the finely orchestrated porous architecture inherent in the P–N–S-Cmph matrix. Remarkably, the P–N–S-Cmph configuration exhibited a commendable inaugural ICE of 70.74%, coupled with an exceptional rate capability and commendable cycling robustness, manifesting a sustained specific capacity of 280 mAh/g at an elevated current density of 2000 mAg over 500 operational cycles Figure 11(c).

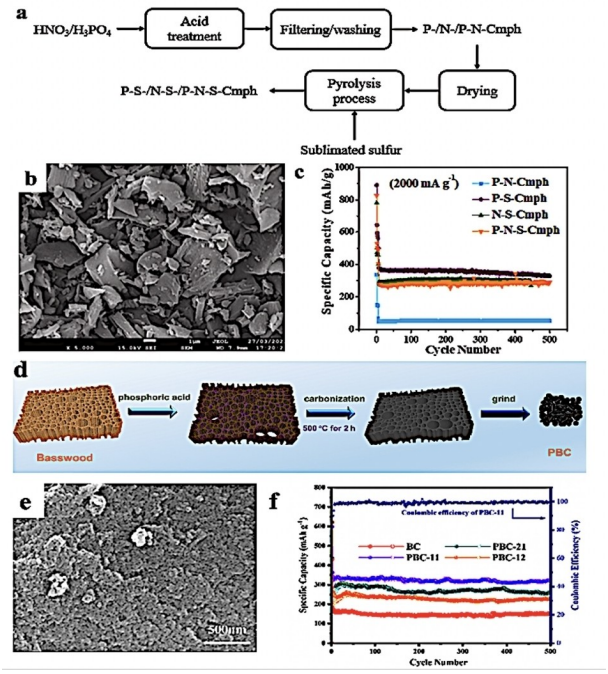

Figure 11. a) Synthesis method and design of resource collection of hierarchical porous hard carbon. b) morphology of synthesized hard carbon from rubber wood sawdust. c) cycling performance for 500 cycles with the corresponding Coulombic efficiencies of C-HC and P-HC electrodes. Adapted from Ref.[147] Copyright (2023) with permission from Elsevier. d) Synthesis route of PBC. e) SEM image of PBC-11. f) capacity chart of PBC-11 for 500 cycles. Adapted from Ref.[148] Copyright (2020) with permission from American Chemical Society.

The remarkable performance metrics of the envisaged anodic substrates can be primarily ascribed to the synergistic interplay facilitated by the heteroatom doping, incorporating sulfur (S), nitrogen (N), and phosphorus (P), thereby engendering an augmented interlayer spacing within the doped-Cmph-HCs. This strategic doping strategy culminates in the provision of an enhanced array of active sites, thereby amplifying the reservoir for Na^+ storage within the host material. Consequently, this endeavor epitomizes a straightforward yet efficacious approach towards the rational design and synthesis of high-performance anode materials tailored specifically for SIB applications. In another study. Xu et. al., used a stable porous carbon in SIB as anode material via phosphoric acid activation Figure 11(d).[148] Three different forms of p-wood porous carbon were synthesized with various mass ratios of phosphoric acid to wood in which each of them showed unique properties. The SEM analysis depicted in Figure 11(e) elucidates the abundant pore structure characteristic of the PBC-11 electrode. Notably, the initial discharge capacity of PBC-11 reaches an impressive 604 mAh/g. Even after 500 cycles at a current density of 0.1 A/g, the discharge capacity remains substantial at 326.3 mAh/g, with Coulombic efficiency of 100%, as illustrated in Figure 11(f). In essence, the amalgamation of low-cost synthesis, high carbon yield, stable cycling performance, and exceptional rate capability renders PBC-11 a formidable candidate as a green anode material for SIBs. This innovation brings the application of sodium-ion batteries in equipment within reach.

Den et al. have achieved a significant breakthrough by developing high-performance carbon materials through successfully engineering of pine-derived carbon. This was achieved by precise doping of carbonyl groups and closed micropores through an innovative combination of sulfuric acid pre-treatment and pre-carbonization. This pioneering approach has enabled the creation of a unique carbon material with enhanced electrochemical properties, characterized by the strategic introduction of carbonyl groups and the deliberate closure of micropores, thereby unlocking its full potential for advanced energy storage applications.[149] The pre-carbonization procedure is elucidated to augment the formation of required enclosed nanocavities (<2 nm), concurrently unveiling a dense anode structure as evidenced by SEM analysis Figure 12(a–e). Consequently, the S-TPHC variant manifests a significantly enhanced Na^+ storage capability attributed to the heightened presence of carbonyl groups and closed micropores. S-TPHC demonstrates an ultra-long cycling lifespan, retaining a capacity of 277 mAh/g at 0.3 A/g over 1000 cycles in the diglyme-based electrolyte. S-TPHC Na_2FePO_4F/C full cell in ether based electrolyte displayed a substantial energy density of 166.2 Wh/kg along with an extended cycle life exceeding 200 cycles at 1 C Figure 12(f and g). This endeavor unveils a novel approach to fabricate sustainable, economically viable, and high-performance biomass-derived carbons tailored for sodium-ion Batteries (SIBs). Doped wood-based anodes for sodium-ion batteries (SIBs) encounter several challenges and drawbacks. One significant issue is the precise control and uniform distribution of dopant elements within the wood matrix, which can be technically challenging and may result in variations in electrochemical performance.

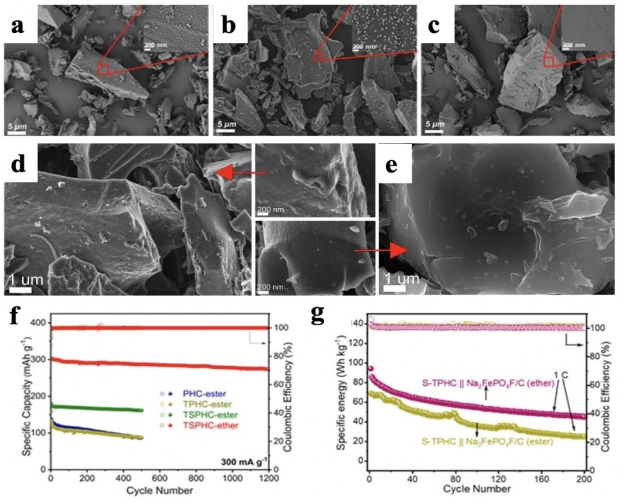

Figure 12. a-c) Scanning Electron Microscope (SEM) images of PHC, TPHC and S-TPHC respectively. d,e) SEM images of S-TPHC-ester electrode and S-TPHC-ether electrode respectively. f) cycling stability of 300 mA/g for PHC-ester, TPHC-ester, S-TPHC-ester, and S-TPHC-ether respectively. g) cycling performance of the full cell at a constant rate of 1 C. Adapted from Ref.[149] Copyright (2021) with permission from American Chemical Society.

Additionally, the compatibility of dopants with the wood substrate and their long-term stability under battery operating conditions need to be carefully evaluated to ensure sustained enhancement of battery performance. The incorporation of dopants may introduce additional processing steps and costs to the fabrication process, potentially impacting the scalability and commercial viability of doped wood-based anodes. The optimization of dopant concentration and composition to achieve the desired electrochemical properties while minimizing adverse effects remains a complex and iterative process. Addressing these challenges is crucial for realizing the full potential of doped wood-based anodes for SIBs and advancing their practical implementation in next-generation energy storage systems.

6.3. Waste Wood-Based Anode

The integration of waste wood-based anodes marks a significant advancement in the realm of sodium-ion batteries (SIBs), presenting a sustainable and innovative approach to energy storage. Waste wood, sourced from various industrial, construction, or agricultural sectors, offers a readily available and underutilized resource that can be repurposed for battery applications. By transforming waste wood into functional anode materials for SIBs, not only can environmental benefits be realized through waste reduction and recycling, but also economic advantages through the utilization of cost-effective feedstock. In order to investigate the formation of mechanisms of closed pores and their effect on sodium storage Tang et al., employed a waste wood-derived carbon as a template[89] Consequently, the cellulose of high crystallinity within wood undergoes decomposition, yielding elongated carbon layers that form the walls of enclosed pores, as evidenced by SEM imagery Figure 13(a–c). The refined specimen showcases exceptional performance metrics, boasting a notable reversible capacity of 430 mAh/g at a rate of 20 mA/g (with a plateau capacity of 293 mAh/g observed for the second cycle), alongside impressive rate capabilities and stable cycling performance (maintaining 85.4% retention after 400 cycles at 500 mA/g) Figure 13(d and e). A comprehensive understanding of the mechanisms governing closed pore formation promises to significantly advance the strategic design of hard carbon anodes endowed with high capacity.

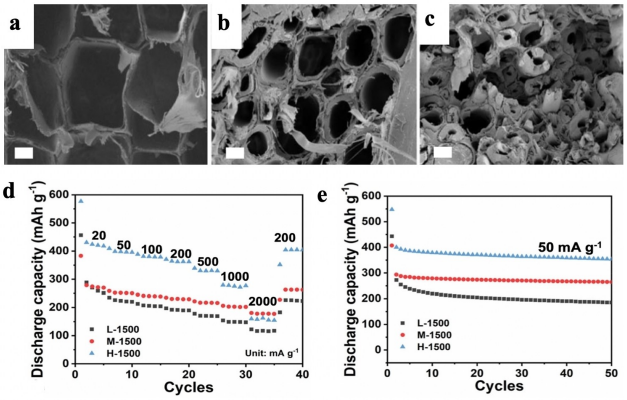

Figure 13. a-c) SEM images of L-wood, M-wood, and H-wood respectively. d) rate. e) cycling performance of hard carbon samples prepared at 155 °C. Adapted from Ref.[89] Copyright (2023) with permission from Nature communications.

While waste wood-based anodes for sodium-ion batteries (SIBs) offer promising environmental and economic benefits, they also face several challenges and drawbacks. One significant concern is the heterogeneous nature of waste wood feedstock, which can lead to variability in the properties of the resulting anode materials, affecting their electrochemical performance and cycling stability. Additionally, the presence of impurities and contaminants in waste wood, such as paints, coatings, or preservatives, may require extensive pre-treatment processes to ensure the purity and integrity of the anode material, increasing production costs and complexity. The structural integrity and mechanical properties of waste wood-based anodes may be compromised during prolonged cycling, leading to performance degradation and reduced lifespan. Addressing these challenges is essential to unlocking the full potential of waste wood-based anodes for SIBs and realizing their role in sustainable energy storage solutions. In conclusion, wood-structured anodes present a promising avenue for sodium-ion batteries (SIBs), offering advantages such as low cost, abundance, and environmental friendliness. The unique microstructure of wood enables efficient sodium-ion storage and transport, leading to enhanced electrochemical performance. Numerous challenges persist, encompassing the need to refine wood processing techniques in order to attain the desired levels of porosity and conductivity enhancing long-term stability and cycling performance. is imperative. Additionally, extensive research is warranted to upscale production processes and evaluate the environmental ramifications of widespread implementation. Despite these challenges, the advancement of wood-structured anodes harbors immense potential for propelling the domain of SIBs and facilitating the achievement of sustainable energy storage solutions.

7. Conclusions and Future Perspectives

The utilization of wood-derived anode materials has emerged as a focal point of considerable interest for prospective deployment in the next-generation of lithium and sodium-ion batteries. Various types of wood have been explored for lithium and sodium-ion battery applications, including pine, birch, oak, poplar, bamboo, and eucalyptus, among others. Each type of wood possesses unique structural and chemical characteristics that influence its suitability as an anode material. Pine, for instance, is abundant and exhibits good mechanical strength, making it a popular choice. Birch wood offers excellent conductivity and stability, while oak boasts high density and potentially enhanced energy storage capacity. Bamboo presents a highly porous structure, facilitating ion diffusion and storage. Poplar wood's porous structure and high carbon content make it an ideal candidate for both lithium-ion and sodium-ion

battery applications due to enhanced ion diffusion and stability. Eucalyptus wood, known for its hardness and durability, may offer improved cycling stability. To determine the "best" type of wood depends on specific battery requirements, such as energy density, power output, and cost-effectiveness, as well as the ease of processing and scalability of the chosen material. Different types of wood have varying characteristics that can affect their suitability for lithium and sodium-ion battery applications. Some key characteristics to consider includes porosity, density, chemical composition, structure, thermal stability, cost and availability as well as thermal stability. Through meticulously controlled carbonization processes, various wood species have been transformed into conductive porous carbon materials, poised for integration into the electrodes of Li-ion and Na-ion batteries. Particularly noteworthy is the electrochemical prowess exhibited by self-standing 3D carbon derived from wood, showcasing remarkable versatility across a diverse array of applications, notably serving as carbon anodes within the realms of Li-ion and Na-ion battery technologies.[150–157] This underscores the exceptional attributes inherent in wood-derived materials, poised to propel electrochemical energy storage toward a more sustainable economic paradigm. Consequently, this enhances the interaction between the anode and electrolyte interface, thereby extending cell lifespan and bolstering power density. While wood-based anode for lithium and sodium-ion batteries (SIBs) offer several advantages, they also have some limitations and drawbacks. These include structural stability such as repeated expansion and contraction of electrode materials. Low capacity in which wood based anode materials shows low lower specific capacities. Limited rate capability with low reaction kinetics. Variability in properties such as wood species and carbonization conditions. Environmental concerns that include concerns related to large scale harvesting for battery production. and compatibility with electrolytes as wood based anode materials exhibit limited compatibility with electrolytes especially those electrolytes that are highly reactive. Addressing these issues require ongoing research and development efforts which is aimed at improving the synthesis methods, optimizing material properties as well as develop an enhanced understanding of the fundamental electrochemical processes that are involved in wood-based anodes for lithium and sodium-ion batteries.

This review highlights the diverse applications of wood in batteries, emphasizing its structured porous architecture as a key advantage. Wood serves as a foundational scaffold for fabricating low-tortuosity, electronically conductive carbonaceous materials. Leveraging wood's structural robustness, these materials function as self-standing electrodes, further enhanced through techniques like heteroatom doping or nanoparticle deposition.[158] The resulting electrodes exhibit high conductivity and low tortuosity, leading to remarkable power densities in systems involving alkali metals like Li and Na. Engineered materials derived from wood have the potential to enhance electrochemical properties, promising exciting advancements in battery technology.[88] This comprehensive assessment must encompass raw material extraction and processing, manufacturing, distribution, utilization, recycling, and ultimate disposal stages. The prospective environmental sustainability advantages inherent in wood-based batteries are succinctly delineated in Figure 14. Presently, wood-based lithium and sodium-ion battery anodes have been engineered to yield heightened energy densities and prolonged life cycles, albeit at the expense of certain Circular Economy principles. Therefore, forthcoming research endeavors should accord paramount importance to factors such as resource and energy efficiency during the carbonization process, process streamlining, and simplification of battery complexity. By addressing these crucial aspects, researchers can not only contribute to the mitigation of environmental impacts associated with battery fabrication but also facilitate the development of more efficient recycling and disposal protocols, thereby promoting a more sustainable and environmentally conscious approach to battery production and management.

As we gaze into the future, it becomes increasingly evident that researchers hold the key to unlock the full potential of wood-based batteries while ensuring their sustainability remains at the forefront of innovation. Beyond mere technological advancements, this journey involves a holistic approach that considers every stage of the battery lifecycle. From the initial extraction of raw materials to the final disposal of used batteries, each step presents an opportunity to minimize environmental impact and maximize resource efficiency. In this pursuit, the optimization of production processes stands as a cornerstone. By refining manufacturing techniques, researchers can not only improve the performance of wood-derived battery components but also reduce energy consumption and waste generation. Additionally, simplifying battery design and operation streamlines manufacturing processes while enhancing user accessibility and usability, thereby democratizing sustainable energy solutions. However, the journey towards sustainability does not end with production. Developing efficient recycling and disposal protocols is equally paramount. By

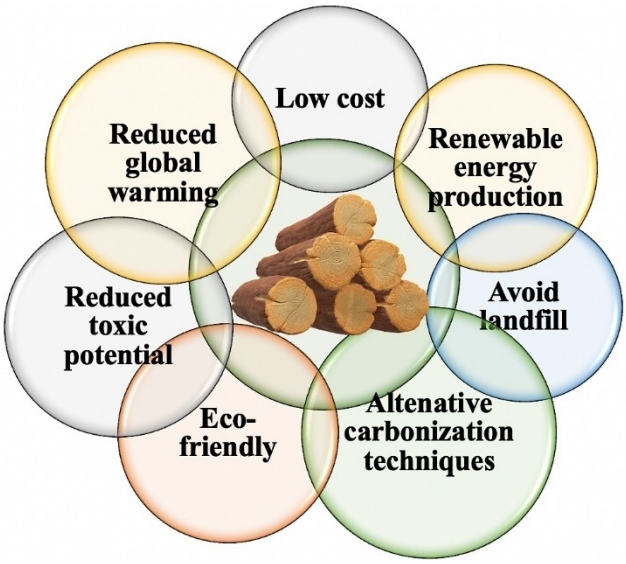

Figure 14. Environmental sustainability benefits arising from wood-based batteries.

implementing closed-loop systems that enable the recovery and reuse of valuable materials from spent batteries, researchers can minimize the environmental footprint of wood-based battery technology. Exploring innovative disposal methods, such as biodegradable components or closed-loop recycling systems, ensures that end-of-life batteries pose minimal harm to the environment. By integrating these multifaceted considerations into future research endeavors, the authors envision a transformative shift towards a more environmentally conscious approach to battery technology. This concerted effort not only fosters a greener and more sustainable future but also inspires a paradigm shift in how we perceive and interact with energy storage solutions. Ultimately, the journey towards sustainability is not just about advancing technology; it's about reimagining our relationship with the planet and charting a course towards a more harmonious coexistence with nature.

Acknowledgements

Financial support from Innovative Research Team of High-level Local Universities in Shanghai and Shanghai Municipal Education Commission.

Conflict of Interests

The authors declare no conflict of interest.

Keywords: Anode materials · Wood derived materials · Energy storage · Lithium-ion batteries · Sodium-ion batteries

[1] M. Abdelbaky, J. R. Peeters, W. Dewulf, *Waste Management* **2021**, *125*, 1–9.
[2] Y. Cao, Y. Sun, C. Guo, W. Sun, Y. Wu, Y. Xu, T. Liu, Y. Wang, *Angew. Chem. Int. Ed.* **2024**, *63*, 2316208.
[3] H. Cavers, P. Molaiyan, M. Abdollahifar, U. Lassi, A. Kwade, *Adv. Energy Mater.* **2022**, *12*, 2200147.
[4] T. Liu, Y. Xu, H. Fang, L. Chen, J. Ying, M. Guo, Y. Wang, Q. Shen, X. Wang, Y. Wang, Z. Yu, *J. Mater. Chem. A* **2024**, *12*, 2283–2293.
[5] A. Crawford, J. Lunde Seefeldt, R. Kent, M. Helbert, G. P. Guzmán, A. González, Z. Chen, A. Abbott, *One Earth* **2021**, *4*, 323–326.
[6] L. Zhao, T. Zhang, W. Li, T. Li, L. Zhang, X. Zhang, Z. Wang, *Eng.* **2023**, *24*, 172–183.
[7] I. Mohan, A. Raj, K. Shubham, D. B. Lata, S. Mandal, S. Kumar, *J. Energy Storage* **2022**, *55*, 105625.
[8] J. Xu, Q. Yin, X. Li, X. Tan, Q. Liu, X. Lu, B. Cao, X. Yuan, Y. Li, L. Shen, Y. Lu, *Nano Lett.* **2022**, *22*, 3054–3061.
[9] O. Okhay, A. Tkach, *Nanomater.* **2021**, *11*, 1240.
[10] P. Molaiyan, G. S. Dos Reis, D. Karuppiah, C. M. Subramaniyam, F. García-Alvarado, U. Lassi, *Batteries* **2023**, *9*, 116.
[11] M. Abdollahifar, P. Molaiyan, M. Perovic, A. Kwade, *Energies (Basel)* **2022**, *15*, 8791.
[12] Y. Cao, Q. Xu, Y. Sun, J. Shi, Y. Xu, Y. Tang, X. Chen, S. Yang, Z. Jiang, H.-D. Um, X. Li, Y. Wang *Proc. Nat. Acad. Sci. USA* **2024**, *121*, 2315407121.
[13] A. Liu, T.-F. Liu, H.-D. Yuan, Y. Wang, Y.-J. Liu, J.-M. Luo, J.-W. Nai, X.-Y. Tao, *New Carbon Mater.* **2022**, *37*, 658–674.
[14] D. Alvira, D. Antorán, J. J. Manyà, *Chem. Eng. J.* **2022**, *447*, 137468.
[15] G. S. dos Reis, R. M. A. Pinheiro Lima, S. H. Larsson, C. M. Subramaniyam, V. M. Dinh, M. Thyrel, H. P. de Oliveira, *J. Environ. Chem. Eng.* **2021**, *9*, 106155.
[16] G. S. dos Reis, H. P. de Oliveira, S. H. Larsson, M. Thyrel, E. Claudio Lima, *Nanomater.* **2021**, *11*, 424.
[17] G. S. dos Reis, S. H. Larsson, H. P. de Oliveira, M. Thyrel, E. Claudio Lima, *Nanomater.* **2020**, *10*, 1398.
[18] X. Lu, Y. Cao, Y. Sun, H. Wang, W. Sun, Y. Xu, Y. Wu, C. Yang, Y. Wang, *Angew. Chem. Int. Ed.* **2024**, *63*, 202320259.
[19] M. González-Hourcade, G. Simões dos Reis, A. Grimm, V. M. Dinh, E. C. Lima, S. H. Larsson, F. G. Gentili, *J. Clean. Prod.* **2022**, *348*, 131280.
[20] Q. Deng, H. Liu, Y. Zhou, Z. Luo, Y. Wang, Z. Zhao, R. Yang, *J. Electroanalytical Chem.* **2021**, *899*, 115668.
[21] S. K. Saju, S. Chattopadhyay, J. Xu, S. Alhashim, A. Pramanik, P. M. Ajayan, *Cell Rep. Phys. Sci.* **2024**, *5*, 101851.
[22] M. M. Abu-Omar, K. Barta, G. T. Beckham, J. S. Luterbacher, J. Ralph, R. Rinaldi, Y. Román-Leshkov, J. S. M. Samec, B. F. Sels, F. Wang, *Energy Environ. Sci.* **2021**, *14*, 262–292.
[23] J. Sun, Z. Wu, C. Ma, M. Xu, S. Luo, W. Li, S. Liu, *J. Mater. Chem. A* **2021**, *9*, 13822–13850.
[24] C. Yang, Q. Wu, W. Xie, X. Zhang, A. Brozena, J. Zheng, M. N. Garaga, B. H. Ko, Y. Mao, S. He, Y. Gao, P. Wang, M. Tyagi, F. Jiao, R. Briber, P. Albertus, C. Wang, S. Greenbaum, Y.-Y. Hu, A. Isogai, M. Winter, K. Xu, Y. Qi, L. Hu, *Nature* **2021**, *598*, 590–596.
[25] Y. Wang, M. Zhang, X. Shen, H. Wang, H. Wang, K. Xia, Z. Yin, Y. Zhang, *Small* **2021**, *17*, 2008079.
[26] C. Chen, L. Hu, *Adv. Mater.* **2021**, *33*, 2002890.
[27] W. Luo, F. Shen, C. Bommier, H. Zhu, X. Ji, L. Hu, *Acc. Chem. Res.* **2016**, *49*, 231–240.
[28] F. Wang, L. Zhang, Q. Zhang, J. Yang, G. Duan, W. Xu, F. Yang, S. Jiang, *Appl. Energy* **2021**, *289*, 116734.
[29] L. Chen, L. Bai, J. Yeo, T. Wei, W. Chen, Z. Fan, *ACS Appl. Mater. Interfaces* **2020**, *12*, 27499–27507.
[30] J. Xu, J. Lei, N. Ming, C. Zhang, K. Huo, *Adv. Funct. Mater.* **2022**, *32*, 2204426.
[31] P. Molaiyan, G. S. Dos Reis, D. Karuppiah, C. M. Subramaniyam, F. García-Alvarado, U. Lassi, *Batteries* **2023**, *9*, 116.
[32] J. Xu, J. Lei, N. Ming, C. Zhang, K. Huo, *Adv. Funct. Mater.* **2022**, *32*, 2204426.
[33] F. Jiang, T. Li, Y. Li, Y. Zhang, A. Gong, J. Dai, E. Hitz, W. Luo, L. Hu, *Adv. Mater.* **2018**, *30*, 1703453.
[34] J. Huang, B. Zhao, T. Liu, J. Mou, Z. Jiang, J. Liu, H. Li, M. Liu, *Adv. Funct. Mater.* **2019**, *29*, 1902255.
[35] T. Zhang, F. Ran, *Adv. Funct. Mater.* **2021**, *31*, 2010041.
[36] A. Kumar Prajapati, A. Bhatnagar, *J. Energy Chem.* **2023**, *83*, 509–540.
[37] Q. Liu, R. Xu, D. Mu, G. Tan, H. Gao, N. Li, R. Chen, F. Wu, *Carbon Energy* **2022**, *4*, 458–479.
[38] J. Li, C. Lin, M. Weng, Y. Qiu, P. Chen, K. Yang, W. Huang, Y. Hong, J. Li, M. Zhang, C. Dong, W. Zhao, Z. Xu, X. Wang, K. Xu, J. Sun, F. Pan, *Nat. Nanotech.* **2021**, *16*, 599–605.
[39] A. Kumar Prajapati, A. Bhatnagar, *J. Energy Chem.* **2023**, *83*, 509–540.
[40] Y. Gao, Z. Pan, J. Sun, Z. Liu, J. Wang, *Nanomicro. Lett.* **2022**, *14*, 94.
[41] D. Wang, C. Han, F. Mo, Q. Yang, Y. Zhao, Q. Li, G. Liang, B. Dong, C. Zhi, *Energy Storage Mater.* **2020**, *28*, 264–292.
[42] A. Manthiram, *Nat. Commun.* **2020**, *11*, 1550.
[43] Y. Yao, Z. Chen, R. Yu, Q. Chen, J. Zhu, X. Hong, L. Zhou, J. Wu, L. Mai, *ACS Appl. Mater. Interfaces* **2020**, *12*, 40648–40654.
[44] Q. Li, X. Yu, H. Li, *eTransportation* **2022**, *14*, 100201.
[45] Y. Shi, Y. Feng, Q. Zhang, J. Shuai, J. Niu, *Energy* **2023**, *262*, 125420.
[46] F. Xie, Z. Xu, Z. Guo, M.-M. Titirici, *Prog. Energy* **2020**, *2*, 042002.
[47] Y.-M. Chang, H.-W. Lin, L.-J. Li, H.-Y. Chen, *Mater. Today. Adv.* **2020**, *6*, 100054.
[48] H. S. Hirsh, Y. Li, D. H. S. Tan, M. Zhang, E. Zhao, Y. S. Meng, *Adv. Energy Mater.* **2020**, *10*, 2001274.
[49] J. Darga, J. Lamb, A. Manthiram, *Energy Tech.* **2020**, *8*, 2000723.
[50] Y. Gao, Z. Pan, J. Sun, Z. Liu, J. Wang, *Nanomicro Lett.* **2022**, *14*, 94.
[51] F. Zhang, B. He, Y. Xin, T. Zhu, Y. Zhang, S. Wang, W. Li, Y. Yang, H. Tian, *Chem. Rev.* **2024**, 728.
[52] H. Bai, Z. Song, *J. Power Sources* **2023**, *580*, 233426.
[53] Q. Wang, J. Hu, T. Yang, S. Chang, *Protoplasma* **2021**, *258*, 361–370.
[54] B. Feng, L. Xu, Z. Yu, G. Liu, Y. Liao, S. Chang, J. Hu, *Electrochem. Commun.* **2023**, *148*, 107439.
[55] W. Wu, Y. Xu, X. Ma, Z. Tian, C. Zhang, J. Han, X. Han, S. He, G. Duan, Y. Li, *Adv. Funct. Mater.* **2023**, *33*, 2302351.
[56] R. Patil, M. Mishra, S. Liu, S. C. Jun, S. Dutta, *Adv. Sustain. Syst.* **2024**, *8*, 2300275.
[57] J. A. Okolie, S. Nanda, A. K. Dalai, J. A. Kozinski, *Waste Biomass Valor.* **2021**, *12*, 2145–2169.

[58] Y. Ding, Z. Pang, K. Lan, Y. Yao, G. Panzarasa, L. Xu, M. Lo Ricco, D. R. Rammer, J. Y. Zhu, M. Hu, X. Pan, T. Li, I. Burgert, L. Hu, *Chem. Rev.* **2023**, *123*, 1843–1888.
[59] P. Wang, G. Zhang, X.-Y. Wei, R. Liu, J.-J. Gu, F.-F. Cao, *J. Am. Chem. Soc.* **2021**, *143*, 3280–3283.
[60] S. Koskela, S. Wang, L. Li, L. Zha, L. A. Berglund, Q. Zhou, *Small* **2023**, *19*, 2205056.
[61] A. T. Hoang, H. C. Ong, I. M. R. Fattah, C. T. Chong, C. K. Cheng, R. Sakthivel, Y. S. Ok, *Fuel Process. Technol.* **2021**, *223*, 106997.
[62] B. Feng, L. Xu, Z. Yu, G. Liu, Y. Liao, S. Chang, J. Hu, *Electrochem. Commun.* **2023**, *148*, 107439.
[63] Y. Liao, S.-F. Koelewijn, G. Van den Bossche, J. Van Aelst, S. Van den Bosch, T. Renders, K. Navare, T. Nicolaï, K. Van Aelst, M. Maesen, H. Matsushima, J. M. Thevelein, K. Van Acker, B. Lagrain, D. Verboekend, B. F. Sels, *Science (1979)* **2020**, *367*, 1385–1390.
[64] B. Feng, L. Xu, Z. Yu, G. Liu, Y. Liao, S. Chang, J. Hu, *Electrochem. Commun.* **2023**, *148*, 107439.
[65] W. Long, B. Fang, A. Ignaszak, Z. Wu, Y.-J. Wang, D. Wilkinson, *Chem. Soc. Rev.* **2017**, *46*, 7176–7190.
[66] H. Wang, C. Wang, B. Dang, Y. Xiong, C. Jin, Q. Sun, M. Xu, *ChemElectroChem* **2018**, *5*, 2367–2375.
[67] Q. Meng, B. Chen, W. Jian, X. Zhang, S. Sun, T. Wang, W. Zhang, *J. Power Sources* **2023**, *581*, 233475.
[68] M. Muddasar, A. Beaucamp, M. Culebras, M. N. Collins, *Int. J. Biol. Macromol.* **2022**, *219*, 788–803.
[69] D. Trache, A. F. Tarchoun, M. Derradji, T. S. Hamidon, N. Masruchin, N. Brosse, M. H. Hussin, *Front. Chem.* **2020**, *8*, 392.
[70] P. G. Marakana, A. Dey, B. Saini, *J. Environ. Chem. Eng.* **2021**, *9*, 106606.
[71] Y. Xu, Z. Wu, A. Li, N. Chen, J. Rao, Q. Zeng, *Polymers (Basel)* **2024**, *16*, 423.
[72] A. Anžlovar, E. Žagar, *Nanomater.* **2022**, *12*, 1837.
[73] J. Wei, Q. Ma, Y. Teng, T. Yang, K. H. Wong, Y. Cui, B. Zheng, D. Li, D. Luo, A. Yu, *Adv. Energy Mater.* **2024**, 2400208.
[74] E. A. Agustiany, M. Rasyidur Ridho, M. D. N. Rahmi, E. W. Madyaratri, F. Falah, M. A. R. Lubis, N. N. Solihat, F. A. Syamani, P. Karungamye, A. Sohail, D. S. Nawawi, A. H. Prianto, A. H. Iswanto, M. Ghozali, W. K. Restu, I. Juliana, P. Antov, L. Kristak, W. Fatriasari, A. Fudholi, *Polym. Compos.* **2022**, *43*, 4848–4865.
[75] M. Mariana, T. Alfatah, A. K. H. P. S., E. B. Yahya, N. G. Olaiya, A. Nuryawan, E. M. Mistar, C. K. Abdullah, S. N. Abdulmadjid, H. Ismail, *J. Mater. Res. Techn.* **2021**, *15*, 2287–2316.
[76] H. Y. Jung, J. S. Lee, H. T. Han, J. Jung, K. Eom, J. T. Lee, *Polymers (Basel)* **2022**, *14*, 673.
[77] J. Zhang, H. Xiang, Z. Cao, S. Wang, M. Zhu, *Green Energy Environ.* **2024**, *9*.
[78] X.-S. Wu, X.-L. Dong, B.-Y. Wang, J.-L. Xia, W.-C. Li, *Renew Energy* **2022**, *189*, 630–638.
[79] J. Zhu, C. Yan, X. Zhang, C. Yang, M. Jiang, X. Zhang, *Prog Energy Combust. Sci.* **2020**, *76*, 100788.
[80] N. Soltani, A. Bahrami, L. Giebeler, T. Gemming, D. Mikhailova, *Prog Energy Combust. Sci.* **2021**, *87*, 100929.
[81] T. Zeng, H. Yang, H. Wang, G. Chen, *J. Phy. Chem. C* **2020**, *124*, 5999–6011.
[82] M. M. Obeid, Q. Sun, *Carbon N. Y.* **2022**, *188*, 95–103.
[83] X. Tang, D. Liu, Y.-J. Wang, L. Cui, A. Ignaszak, Y. Yu, J. Zhang, *Prog. Mater. Sci.* **2021**, *118*, 100770.
[84] G. Zhang, X. Liu, L. Wang, H. Fu, *J. Mater. Chem. A.* **2022**, *10*, 9277–9307.
[85] S. Parida, D. P. Dutta, *ACS* **2022**, 307–366.
[86] S. Chen, L. Qiu, H.-M. Cheng, *Chem. Rev.* **2020**, *120*, 2811–2878.
[87] B. Yan, J. Zheng, L. Feng, Q. Zhang, C. Zhang, Y. Ding, J. Han, S. Jiang, S. He, *Mater. Des.* **2023**, *229*, 111904.
[88] C. Chen, Y. Kuang, S. Zhu, I. Burgert, T. Keplinger, A. Gong, T. Li, L. Berglund, S. J. Eichhorn, L. Hu, *Nat. Rev. Mater.* **2020**, *5*, 642–666.
[89] Z. Tang, R. Zhang, H. Wang, S. Zhou, Z. Pan, Y. Huang, D. Sun, Y. Tang, X. Ji, K. Amine, M. Shao, *Nat. Commun.* **2023**, *14*, 6024.
[90] A. Kumar, T. Jyske, M. Petrič, *Adv. Sustain. Syst.* **2021**, *5*, 2000251.
[91] Q. Chen, J. Jin, M. Song, X. Zhang, H. Li, J. Zhang, G. Hou, Y. Tang, L. Mai, L. Zhou, *Adv. Mater.* **2022**, *34*, 2107992.
[92] X. Guo, J. Zhang, L. Yuan, B. Xi, F. Gao, X. Zheng, R. Pan, L. Guo, X. An, T. Fan, S. Xiong, *Adv. Energy Mater.* **2023**, *13*, 204376.
[93] T. Farid, M. I. Rafiq, A. Ali, W. Tang, *EcoMat.* **2022**, *4*, 12154.
[94] P. Chaudhary, S. Bansal, B. B. Sharma, S. Saini, A. Joshi, *J. Energy Storage* **2024**, *78*, 109996.
[95] M. Hua, S. Wu, Y. Jin, Y. Zhao, B. Yao, X. He, *Adv. Mater.* **2021**, *33*, 2100983.
[96] J. Wu, Z. Ju, X. Zhang, A. C. Marschilok, K. J. Takeuchi, H. Wang, E. S. Takeuchi, G. Yu, *Adv. Mater.* **2022**, *34*, 2202780.
[97] M. Weiss, R. Ruess, J. Kasnatscheew, Y. Levartovsky, N. R. Levy, P. Minnmann, L. Stolz, T. Waldmann, M. Wohlfahrt-Mehrens, D. Aurbach, M. Winter, Y. Ein-Eli, J. Janek, *Adv. Energy Mater.* **2021**, *11*, 2101126.
[98] A. B. Resing, C. Fukuda, J. G. Werner, *Adv. Mater.* **2023**, *35*, 2209694.
[99] R. He, G. Tian, S. Li, Z. Han, W. Zhong, S. Cheng, J. Xie, *Nano Lett.* **2022**, *22*, 2429–2436.
[100] Z. Zhang, Z. Wang, L. Zhang, D. Liu, C. Yu, X. Yan, J. Xie, J. Huang, *Adv. Sci.* **2022**, *9*, 2200744.
[101] T. Zhou, H. Liu, *Mater.* **2022**, *15*, 1598.
[102] G. G. Mastantuoni, V. C. Tran, I. Engquist, L. A. Berglund, Q. Zhou, *Adv. Mater. Interfaces* **2023**, *10*, 2201597.
[103] P. Molaiyan, G. S. Dos Reis, D. Karuppiah, C. M. Subramaniyam, F. García-Alvarado, U. Lassi, *Batteries* **2023**, *9*, 116.
[104] D. Li, H. Guo, S. Jiang, G. Zeng, W. Zhou, Z. Li, *New J. Chem.* **2021**, *45*, 19446–19455.
[105] N. Kumar, P. K. Pathak, R. R. Salunkhe, *Nanoscale* **2023**, *15*, 13740–13749.
[106] Z. Liang, J. Shen, X. Xu, F. Li, J. Liu, B. Yuan, Y. Yu, M. Zhu, *Adv. Mater.* **2022**, *34*, 2200102.
[107] X. Wen, J. Luo, K. Xiang, W. Zhou, C. Zhang, H. Chen, *Chem. Eng. J.* **2023**, *458*, 141381.
[108] B. Escobar, D. C. Martínez-Casillas, K. Y. Pérez-Salcedo, D. Rosas, L. Morales, S. J. Liao, L. L. Huang, X. Shi, *Int. J. Hydrogen Energy* **2021**, *46*, 26053–26073.
[109] J. D. McBrayer, C. A. Apblett, K. L. Harrison, K. R. Fenton, S. D. Minteer, *Nanotechnology* **2021**, *32*, 502005.
[110] T.-T. Nguyen, A. Demortière, B. Fleutot, B. Delobel, C. Delacourt, S. J. Cooper, *NPJ Comput. Mater.* **2020**, *6*, 123.
[111] Y. Wang, W. Yang, C. Zhang, X. Han, J. Han, S. He, J. Hu, S. Jiang, *Ind. Crops Prod.* **2023**, *198*, 116664.
[112] M. Drews, J. Büttner, M. Bauer, J. Ahmed, R. Sahu, C. Scheu, S. Vierrath, A. Fischer, D. Biro, *ChemElectroChem* **2021**, *8*, 4750–4761.
[113] T. Liu, R. Luo, W. Qiao, S.-H. Yoon, I. Mochida, *Electrochim. Acta* **2010**, *55*, 1696–1700.
[114] D. Kang, H.-K. Kim, H.-J. Kim, Y. Han, *J. Alloys Compd.* **2022**, *900*, 163420.
[115] R. A. Adams, A. D. Dysart, R. Esparza, S. Acuña, S. R. Joshi, A. Cox, D. Mulqueen, V. G. Pol, *Ind. Eng. Chem. Res.* **2016**, *55*, 8706–8712.
[116] C. Yang, Q. Gao, W. Tian, Y. Tan, T. Zhang, K. Yang, L. Zhu, *J. Mater. Chem. A* **2014**, *2*, 19975–19982.
[117] Y. Li, H. Zhu, F. Shen, J. Wan, X. Han, J. Dai, H. Dai, L. Hu, *Adv. Funct. Mater.* **2014**, *24*, 7366–7372.
[118] M. Drews, J. Büttner, M. Bauer, J. Ahmed, R. Sahu, C. Scheu, S. Vierrath, A. Fischer, D. Biro, *ChemElectroChem* **2021**, *8*, 4750–4761.
[119] Q. Huang, J. Hu, M. Zhang, M. Li, T. Li, G. Yuan, Y. Liu, X. Zhang, X. Cheng, *Chinese Chem. Lett.* **2022**, *33*, 1091–1094.
[120] J. Revathi, A. Jyothirmayi, T. N. Rao, A. S. Deshpande, *Glob. Challeng.* **2020**, *4*, 1900048.
[121] W. Zhang, Y. Xu, H. Li, C. Wang, B. Qin, Z. Li, Y. Chen, K. Jiang, H. Zhang, *J. Electroanal. Chem.* **2020**, *856*, 113654.
[122] W. He, H. Luo, P. Jing, H. Wang, C. Xu, H. Wu, Q. Wang, Y. Zhang, *J. Alloys. Compd.* **2022**, *918*, 165364.
[123] X. Wang, X. Liu, X. Ren, K. Luo, W. Xu, Q. Hou, W. Liu, *Ind. Crops. Prod.* **2020**, *158*, 113022.
[124] L. Lu, Y. Lu, Z. Xiao, T. Zhang, F. Zhou, T. Ma, Y. Ni, H. Yao, S. Yu, Y. Cui, *Adv. Mater.* **2018**, *30*, 1706745.
[125] Y. Kuang, C. Chen, G. Pastel, Y. Li, J. Song, R. Mi, W. Kong, B. Liu, Y. Jiang, K. Yang, L. Hu, *Adv. Energy Mater.* **2018**, *8*, 1802398.
[126] Q. Huang, J. Hu, M. Zhang, M. Li, T. Li, G. Yuan, Y. Liu, X. Zhang, X. Cheng, *Chin. Chem. Lett.* **2022**, *33*, 1091–1094.
[127] S. Wu, Y. Jin, D. Wang, Z. Xu, L. Li, X. Zou, M. Zhang, Z. Wang, H. Yang, *J. Energy Storage* **2023**, *68*, 107731.
[128] J. Revathi, A. Jyothirmayi, T. N. Rao, A. S. Deshpande, *Glob. Challeng.* **2020**, *4*, 1900048.
[129] W. Zhang, Y. Xu, H. Li, C. Wang, B. Qin, Z. Li, Y. Chen, K. Jiang, H. Zhang, *J. Electroanal. Chem.* **2020**, *856*, 113654.
[130] W. He, H. Luo, P. Jing, H. Wang, C. Xu, H. Wu, Q. Wang, Y. Zhang, *J. Alloys. Compd.* **2022**, *918*, 165364.
[131] X. Wang, X. Liu, X. Ren, K. Luo, W. Xu, Q. Hou, W. Liu, *Ind. Crops. Prod.* **2020**, *158*, 113022.

[132] Z. Song, G. Zhang, X. Deng, Y. Tian, X. Xiao, W. Deng, H. Hou, G. Zou, X. Ji, *Adv. Funct. Mater.* **2022**, *32*, 2205453.
[133] J. Xu, B. Chen, B. Hu, Y. Gu, X. Li, Y. Liu, D. Sha, J. Zhang, S. Huang, *J. Energy Storage* **2024**, *81*, 110306.
[134] J. Xu, B. Chen, B. Hu, Y. Gu, X. Li, Y. Liu, D. Sha, J. Zhang, S. Huang, *J. Energy Storage* **2024**, *81*, 110306.
[135] S. Zhou, Z. Tang, Z. Pan, Y. Huang, L. Zhao, X. Zhang, D. Sun, Y. Tang, A. S. Dhmees, H. Wang, *SusMat.* **2022**, *2*, 357–367.
[136] N. T. Aristote, Z. Song, W. Deng, H. Hou, G. Zou, X. Ji, *J. Power Sources* **2023**, *558*, 232517.
[137] Z. Xu, Y. Huang, L. Ding, J. Huang, H. Gao, T. Li, *Energy Fuels* **2020**, *34*, 11565–11573.
[138] W. Deng, Y. Cao, G. Yuan, G. Liu, X. Zhang, Y. Xia, *ACS Appl. Mater. Interfaces* **2021**, *13*, 47728–47739.
[139] Z. Tang, R. Zhang, H. Wang, S. Zhou, Z. Pan, Y. Huang, D. Sun, Y. Tang, X. Ji, K. Amine, M. Shao, *Nat. Commun.* **2023**, *14*, 6024.
[140] F. Shen, W. Luo, J. Dai, Y. Yao, M. Zhu, E. Hitz, Y. Tang, Y. Chen, V. L. Sprenkle, X. Li, L. Hu, *Adv. Energy Mater.* **2016**, *6*, 1600377.
[141] L. Han, J. Wang, X. Mu, C. Liao, W. Cai, Z. Zhao, Y. Kan, W. Xing, Y. Hu, *Nanoscale* **2020**, *12*, 14642–14650.
[142] Y. Zheng, Y. Lu, X. Qi, Y. Wang, L. Mu, Y. Li, Q. Ma, J. Li, Y.-S. Hu, *Energy Storage Mater.* **2019**, *18*, 269–279.
[143] F. Shen, H. Zhu, W. Luo, J. Wan, L. Zhou, J. Dai, B. Zhao, X. Han, K. Fu, L. Hu, *ACS Appl. Mater. Interfaces* **2015**, *7*, 23291–23296.
[144] W. Jing, M. Wang, Y. Li, H.-R. Li, H. Zhang, S. Hu, H. Wang, Y.-B. He, *Electrochim Acta* **2021**, *391*, 139000.
[145] Y. Chen, Y. Wu, Y. Liao, Z. Zhang, S. Luo, L. Li, Y. Wu, Y. Qing, *J. Power Sources* **2022**, *546*, 231993.
[146] S. Zhou, Z. Tang, Z. Pan, Y. Huang, L. Zhao, X. Zhang, D. Sun, Y. Tang, A. S. Dhmees, H. Wang, *SusMat.* **2022**, *2*, 357–367.
[147] N. T. Aristote, Z. Song, W. Deng, H. Hou, G. Zou, X. Ji, *J. Power Sources* **2023**, *558*, 232517.
[148] Z. Xu, Y. Huang, L. Ding, J. Huang, H. Gao, T. Li, *Energy Fuels* **2020**, *34*, 11565–11573.
[149] W. Deng, Y. Cao, G. Yuan, G. Liu, X. Zhang, Y. Xia, *ACS Appl. Mater. Interfaces* **2021**, *13*, 47728–47739.
[150] B. Sun, Q. Zhang, W. Xu, R. Zhao, C. Zhang, J. Guo, H. Zhu, G. Yuan, W. Lv, X. Li, N. Yang, *Carbon N. Y.* **2023**, *201*, 776–784.
[151] H. Tonnoir, D. Huo, R. L. S. Canevesi, V. Fierro, A. Celzard, R. Janot, *Mater. Today Chem.* **2022**, *23*, 100614.
[152] A. Gomez-Martin, J. Martinez-Fernandez, M. Ruttert, M. Winter, T. Placke, J. Ramirez-Rico, *Chem. Mater.* **2019**, *31*, 7288–7299.
[153] W. Luo, C. Bommier, Z. Jian, X. Li, R. Carter, S. Vail, Y. Lu, J.-J. Lee, X. Ji, *ACS Appl. Mater. Interfaces* **2015**, *7*, 2626–2631.
[154] M. Dahbi, M. Kiso, K. Kubota, T. Horiba, T. Chafik, K. Hida, T. Matsuyama, S. Komaba, *J. Mater. Chem. A* **2017**, *5*, 9917–9928.
[155] R. Muruganantham, F.-M. Wang, W.-R. Liu, *Electrochim Acta* **2022**, *424*, 140573.
[156] Y. Zhu, M. Chen, Q. Li, C. Yuan, C. Wang, *Carbon N. Y.* **2018**, *129*, 695–701.
[157] M. Liu, J. Zhang, S. Guo, B. Wang, Y. Shen, X. Ai, H. Yang, J. Qian, *ACS Appl. Mater. Interfaces* **2020**, *12*, 17620–17627.
[158] I. Gomez, E. Lizundia, *Adv. Sustain. Syst.* **2021**, *5*, 2100236.

Manuscript received: May 5, 2024
Revised manuscript received: June 21, 2024
Accepted manuscript online: July 14, 2024
Version of record online: September 9, 2024